Itaconate and derivatives reduce interferon response and inflammation in influenza A virus infection

Aaqib Sohail[1,9*], Azeem A. Iqbal[1,9*], Nishika Sahini[1,9*], Mohamed Tantawy[1,9], Moritz Winterhoff[1,9], Thomas Ebensen[2] , Robert Geffers[3], Klaus Schughart[4], Fangfang Chen[1,9], Matthias Preusse[1,2], Marina C. Pils[5], Carlos A. Guzman[2], Ahmed Mostafa[6], Stephan Pleschka[6], Christine Falk[7], Alessandro Michelucci[8], Frank Pessler[1,9,**]

[1]Biomarkers for Infectious Diseases, [2]Vaccinology and Applied Microbiology, [3]Genome Analytics, [4]Infection Genetics, [5]Mouse Pathology Platform, Helmholtz Centre for Infection Research, 31824 Braunschweig, Germany

[6]Institute for Medical Virology, Justus-Liebig-University, 35392 Giessen, Germany

[7]Department of Transplantation Immunology, Hannover Medical School, 30625 Hannover, Germany

[8]Dept. of Oncology, Luxembourg Institute of Health, 1526 Luxembourg

[9]TWINCORE Centre for Experimental and Clinical Infection Research, 30625 Hannover, Germany

*Joint first authors

**Corresponding author

Frank Pessler, MD, PhD

Tel. +49 511 220027-167, Mobile +49 160 9728 0364

frank.pessler@twincore.de

Total character count 59381

Abstract

Itaconate has recently emerged as a metabolite with immunomodulatory properties. We evaluated effects of endogenous itaconate and exogenous itaconate, dimethyl-, and 4-octyl-itaconate on host responses to influenza A virus infection. Infection induced *ACOD1* (the enzyme that catalyzes itaconate synthesis) mRNA in monocytes and macrophages, which correlated with viral replication and was abrogated by itaconate treatment. Weight loss and pulmonary inflammation were greater in *Acod1*$^{-/-}$ than wild-type mice. Investigations in cell lines, human lung tissue, and peripheral blood mononuclear cells revealed that the compounds reversed infection-triggered interferon responses and pro-inflammatory gene expression. Ectopic synthesis of itaconate in epithelial cells also reduced inflammation. Single-cell RNA sequencing of PBMC showed that infection induced *ACOD1* exclusively in monocytes, whereas dimethyl-itaconate treatment silenced IFN-responses in monocytes, lymphocytes, and natural killer cells. Viral replication did not increase under itaconate and dimethyl-itaconate treatment despite the dramatically repressed IFN responses, but 4-octyl itaconate inhibited viral transcription in PBMC. The results reveal the potential of itaconate derivatives as adjunct treatments for deleterious host responses in infection by influenza viruses and potentially other viral pathogens.

Key words: innate immunity - influenza virus – pneumonia – single cell RNA sequencing - treatment.

Introduction

As exemplified by influenza viruses (Ramos & Fernandez-Sesma, 2015) and pathogenic coronaviruses (Ragab et al., 2020), overshooting host inflammation, oxidative stress and cell damage/death are major determinants of morbidity and mortality in severe viral infections of humans. Consequently, there is a great need for adjunct treatments that can be given in conjunction with direct-acting anti-virals, with the aim to modulate the host response in such a way that end-organ damage is reduced and clinical outcome is improved.

Itaconic acid initially attracted great interest in the field of biotechnology due to its highly reactive double bonds, which make it an efficient intermediate in the biosynthesis of industrial polymers (reviewed in (Cordes et al., 2015)). The discoveries that its synthesis is highly induced during macrophage activation (Strelko et al., 2011) and that *immune response gene 1* (*Irg1,* since then renamed *aconitate decarboxylase*) encodes the enzyme cis-aconate decarboxylase (ACOD1 in humans, CAD in other organisms), which converts cis-aconitate to itaconate (Chen et al., 2019, Michelucci et al., 2013), have triggered intense efforts to elucidate functions of the endogenous ACOD1/itaconate axis in inflammation and infection. The early recognition that itaconate possesses anti-inflammatory and immunomodulatory properties also suggested that itaconate and prodrugs derived from it may have potential as immunomodulatory and cytoprotective interventions for inflammation-driven diseases (reviewed in (Hooftman & O'Neill, 2019, O'Neill & Artyomov, 2019)).

Most evidence of anti-inflammatory and immunomodulatory effects of itaconate has actually been obtained by treating cells or small animals with chemically modified variants that are presumably taken up more efficiently. 4-Octyl-itaconate (4OI) contains an added 8-carbon chain and acts primarily through activation of the NRF2 pathway (Mills 2018). It has, for instance, shown cytoprotective and anti-inflammatory effects in a variety of models, including lipopolysaccharide (LPS)-induced macrophage activation and LPS-induced sepsis in mice (Mills 2018), in a neuronal model of oxidative stress (Liu 2018), and in peripheral blood mononuclear cells (PBMC) from patients with systemic lupus erythematosus (Tang 2018). Dimethyl-itaconate (DI) has also been shown to exert NRF2 independent anti-inflammatory effects by inhibiting IκBζ activity (Bambouskova 2018). Furthermore, DI possesses cytoprotective effects, which was, for instance, shown by reduced cell damage in mouse models of cardiac ischemia

(Lampropoulou 2016). However, cytoprotective properties have also been demonstrated for unmodified itaconate, notably in a rat model of cerebral ischemic-reperfusion injury (Cordes 2020). Both compounds likely exert cytoprotective effects by reducing reactive oxygen species (ROS) generation via inhibition of succinate dehydrogenase (Cordes 2020, Cordes 2016, Lampropoulou 2016). Considering these varied effects of itaconate and derivatives, it is not surprising that administration of DI has demonstrated beneficial effects in a variety of mouse models of infection-associated inflammation such as LPS-induced mastitis (Zhao 2019) and endometritis (Xu 2020b), and fungal keratitis (Gu 2020). Following early evidence that *Acod1* transcription is strongly induced in severe influenza A virus (IAV) infection in mice (Preusse 2013), its impact on host susceptibility to viral infections has also been studied, and protective effects of itaconate on neurons exposed to RNA viruses have been reported (Cho 2013, Daniels 2019). On the other hand, in a recent study using a mouse model of IAV infection, deleting the *Acod1* locus did not affect weight loss or survival, whereas it clearly worsened the outcome of *Mycobacterium tuberculosis* infection in the same mouse strain (Nair 2018). This lack of effect on IAV infection was surprising because abnormally increased inflammation is usually asociated with deleterious effects on the host during viral infections. For instance, it has been shown that overactive inflammatory responses are associated with decreased survival and increased weight loss in IAV infected inbred mouse strains (Alberts, Srivastava et al., 2010). While the role of endogenous itaconate in protection from viral infections thus remains incompletely understood, the above results do suggest a strong potential of external application of itaconate or its derivatives to ameliorate inflammation and other deleterious consequences of viral infections.

Focusing on IAV as one of the most important human respiratory viral pathogens (Collaborators, 2018), we therefore examined role and regulation of the endogenous ACOD1/itaconate axis in a mouse model of IAV infection and subsequently performed a detailed analysis of the modulatory effects of exogenous addition of itaconate and derivatives on inflammatory responses in IAV-infected human cell lines, explanted lung tissue, and PBMC, both at the bulk and single-cell levels. We find that loss of ACOD1 and itaconate synthesis led to increased inflammation during infection and that exogenous itaconate, DI, and 4OI substantially reduced inflammation, most notably IFN responses, without enhancing viral replication. 4OI was unique in that it also exerted a direct anti-viral effect.

Results

***Acod1* expression and itaconate synthesis are induced in mouse lung during IAV-infection and limit pulmonary inflammation and disease severity.** Compared with C57BL/6J, DBA/2J mice are more susceptible to IAV infection in that weight loss is more rapid, mortality is higher, and inflammation is more pronounced (Preusse 2017, Srivastava 2009). We have shown previously that *Acod1* transcription in the first 48 h of infection is higher in IAV-infected lung from DBA/2J than from C57BL/6J mice (Preusse 2013). A reanalysis of our RNAseq data from a longer time course (Wilk 2015) showed that this difference persisted at least through day 3 post infection (p.i.) and that *Acod1* expression nearly normalized by day 14 in the surviving strain (**Fig. 1A**). This analysis also revealed a remarkable correlation with expression of *Tnfaip3* (encoding an anti-inflammatory deubiquitinase) and a weaker positive correlation with *Hmox1* and *2* (encoding inducible anti-oxidant enzymes), all of which are known to be co-regulated with *Acod1* (Li, Zhang et al., 2013, Uddin, Joe et al., 2016). *Acod1* was the 4th most highly upregulated pulmonary mRNA 48 h p.i. in C57BL/6J mice, where it appeared in a cluster of transcripts pertaining to IFN responses and innate immunity (**Fig. 1B**). These results underscored the close association of *Acod1* expression with systemic inflammation and oxidative stress in IAV-infected mice. We therefore tested whether targeted deletion of *Acod1* would affect inflammatory responses and host susceptibility to IAV infection. Itaconate was not detectable in lungs from IAV-infected *Acod1*$^{-/-}$ mice; it was highly elevated on days 7/8 p.i. in the *Acod1*$^{+/+}$ and, significantly less, in *Acod1*$^{+/-}$ mice, and returned to normal by day 14 (**Fig. 1C**). Both weight loss and mortality were higher in *Acod1*$^{-/-}$ than *Acod*$^{+/+}$ female C57BL/6J mice (**Fig. 1D,E**), with greatest changes occurring around day 8, the time of maximal itaconate accumulation. Histologically assessed pulmonary inflammation was greatest in *Acod1*$^{-/-}$ mice and intermediate in *Acod1*$^{+/-}$ mice (**Fig. 1F**). Thus, itaconate synthesis correlated with disease activity, and loss of *Acod1* was associated with more severe disease and higher pulmonary inflammation.

IAV infection induces *ACOD1* expression in human PBMC and macrophages. Unless stated otherwise, all infections human cells and tissue were done using the strain PR8M (A/PuertoRico/8/34 H1N1). We first tested whether IAV infection increased *ACOD1* mRNA levels in human PBMC and M1/M2 macrophages. Phorbol myristate acetate (PMA)-

differentiated THP-1 (dTHP-1) cells were analyzed for comparison. Viral transcription, as measured by hemagglutinin (*HA*) mRNA levels, was highest in M2 cells (**Fig. 2A**). The strongest *ACOD1* induction was seen in M2 cells and undifferentiated PBMC, and the weakest in M1 cells and dTHP-1 cells (**Fig. 2B-E**), even though the latter two cell types did support a significant degree of viral transcription (**Fig. 2A,D**). As in IAV-infected mouse lung (**Fig. 1**), *TNFAIP3* and *ACOD1* transcriptional correlated with each other (**Fig. 2C**). Infection of dTHP-1 cells with three IAV (H1N1) strains of differential replication efficiency (Petersen, Mostafa et al., 2018b) showed the strongest *ACOD1* and *TNFAIP3* induction by the two strains with the highest and the weakest by the strain with the lowest replication efficiency (**Fig. 2D,E**). Thus, the extent of *ACOD1* induction after IAV infection differed significantly among the cell types tested, was strongest in M2 primary cells, was accompanied in all cases by an increase in *TNFAIP3* mRNA, and correlated with viral replication.

Itaconate and DI markedly reduce IFN responses in dTHP-1 cells without affecting viral RNA replication. We then tested whether these compounds could modulate cellular inflammation due to IAV infection. In infected dTHP-1 cells, treatments with itaconate or DI did not affect viral hemagglutinin (*HA)* mRNA expression, but both reduced induction of *CXCL10*, a key pro-inflammatory chemokine during influenza virus infection, with DI being several-fold more potent (**Fig. 3B,C, Fig. S1**). The 12 h time point was chosen because our previous work had identified it as the peak of IFN-I responses at the mRNA level in IAV-infected dTHP-1 cells (Petersen, Mostafa et al., 2018a). We then assessed global effects of itaconate and DI on cellular gene mRNA expression. A comparison of differentially expressed genes (DEGs) suggested that the two compounds had both shared and unique effects on gene expression (**Fig. 3D**). Both compounds had considerable effects on gene expression in uninfected cells (**Fig. 3E,F**). As expected, IAV infection of untreated cells caused a major induction of IFN-regulated transcripts by 12 h p.i. (see mRNAs labeled in the volcano plot in **Fig. 3G**). Strikingly, addition of both itaconate and DI led to global down-regulation of IFN-regulated genes. This was accompanied by upregulation of a substantial number of other transcripts, indicating that the compounds also modulated other cellular processes (**Fig. 3H,I)**. A principle component analysis (PCA) indicated that effects of the compounds on the cells were so pronounced at these concentrations that treated infected and treated uninfected cells clustered closely together, but far away from

untreated infected or uninfected cells (**Fig. S2**). Indeed, a hierarchical clustering analysis revealed an across-the-board normalization of a clade of IFN- and inflammation-related transcripts by the compounds, but also clusters of DEGs that were upregulated by either or both compounds with respect to both uninfected and infected cells, further indicating effects upon cell homeostasis in general (**EV1A,B**). mRNA and protein expression may be differentially affected by IAV infection due to virus-induced "host-cell shut-off". We therefore assessed release of inflammation-related polypeptides in supernatants from the same experiment (**Fig. 3J**). This analysis confirmed the downregulation of pro-inflammatory factors (e.g., IP-10, MCP-1) by itaconate and DI, but also showed increased IL-8 (DI only) and minor increases of IL1B (both IA and DI) in uninfected cells. Of note, both compounds also increased levels of the anti-inflammatory IL1 receptor antagonist (IL1RA) in supernatants from both infected and uninfected cells. A comprehensive view of the protein targets that were detected by this assay revealed that the two compounds effected substantially different changes in the target cells, as several factors were induced even in uninfected cells specifically by DI or itaconate (**EV2**). Thus, itaconate and DI apparently act on macrophages to release different recruitment programs that modify local inflammatory cell populations.

Analysis of enriched GO terms revealed that IFN-I signaling was strongly induced in the infected cells, which was prevented by treatment with itaconate and DI (**Fig. 4**). This analysis also revealed that both compounds activated metabolic processes, whereas itaconate also modulated processes relating to differentiation and membrane signaling. A KEGG pathway analysis additionally revealed induction of classic pro-inflammatory pathways such as *TNF signaling*, *TLR receptor signaling*, and *chemokine signaling* by infection, all of which were depleted by itaconate and DI treatment (**Fig. S3).** However, in a separate experiment, there were only tendencies of IA and DI to reduce nuclear localization of NF-kB during infection, whereas reduction by 4OI was significant. (**EV1C**). Taken together, these results revealed strong anti-IFN and anti-inflammatory effects of itaconate and DI, but also suggested that they exert other important effects on cell metabolism and differentiation, some of which differ between the compounds.

Anti-inflammatory effects of ectopically expressed itaconate, and exogenous itaconate and DI on IAV-infected respiratory epithelial cells. We then tested whether the effects of itaconate and DI could also be seen in cells not endogenously expressing *ACOD1*. For this purpose, we studied the respiratory epithelial cell line A549, which supports productive IAV infection and does not express *ACOD1*. As expected, infection of A549 cells did not result in induction of *ACOD1* mRNA, but transient transfection with an *ACOD1*-expressing plasmid led to significant *ACOD1* mRNA expression (**Fig. 5A**), which was accompanied by appearance of substantial concentrations of IA (**Fig. 5B**). While there was no effect on viral *HA* mRNA expression, transfection with the *ACOD1*-expressing vector led to a marked reduction in infection-associated *CXCL10* induction (**Fig. 5C,D**). A preliminary treatment experiment showed that (as opposed to THP-1 cells) DI was cytotoxic at 1.0 mM in A549 cells, and the 0.5 mM concentration was therefore used. Treatment with DI resulted in a modest reduction of *HA* expression early in infection and a marked reduction of *CXCL10*, *IL6*, and *IFNB* expression (**Fig. 5E-H**). Exogenous itaconate, too, reduced *CXCL10* mRNA, but less efficiently (**Fig. S4**). Taken together, these results obtained with A549 cells suggest that immunomodulatory effects of itaconate and DI are independent of the ability of the cell type to express endogenous *ACOD1*, and that similar effects on IFN-directed gene expression can be obtained with ectopic, endogenous synthesis of itaconate and exogenously added itaconate and DI.

Next, we assessed effects of itaconate and DI on cellular transcriptomes in IAV-infected A549 cells. PCA revealed the expected normalization of gene expression due to DI treatment, but also increasing effects of the compounds on overall cell homeostasis (**Fig. S5**). As in THP-1 cells, hierarchical clustering analysis revealed clear clustering of each of the four groups and the close relationship of the uninfected and DI-treated infected cells (**EV3**). However, the anti-inflammatory effect of itaconate was weaker than that of DI, and at the higher (40 mM) concentration, the itaconate signature became so dominant that the itaconate-treated infected group now formed its own clade (**Fig. S6)**. IAV infection enriched GO terms related to IFN-I and –II responses as well as other antiviral and pro-inflammatory terms, which could all be reduced to near baseline by treatment with DI or itaconate (**Fig. 6**). Visualization of differentially expressed IFN-related mRNA also showed that, in spite of its overall lower effect on pro-inflammatory signaling than DI, itaconate treatment at the lower (20 mM) concentration did have

a considerable impact on IFN-I expression (**Fig 6B**). In addition, itaconate uniquely inhibited *NFKB signaling* and *fatty acid metabolism*. KEGG-pathway analysis additionally revealed depletion of other pro-inflammatory pathways, including *TNF signaling* and *necroptosis*, by the treatments (**Fig. S7**).

Anti-inflammatory effect of itaconate and DI in a human lung tissue explant (HLTE) model of IAV infection. To test whether the *ACOD1*/itaconate axis and the anti-inflammatory effects of itaconate and DI are functional in the end-organ of IAV infection in humans, we then used a human lung tissue culture model. Indeed, infection with IAV led to brisk transcription of viral *HA* and host *CXCL10* mRNA in a 72 h time course (**Fig. S8**), whereas *ACOD1* mRNA levels did not change significantly. Adding itaconate and DI reduced expression of *CXCL10* mRNA in tissue and IP10 protein in culture supernatant, and itaconate additionally reduced ISG15 mRNA in tissue, whereas viral titers in the supernatant were unaffected (**Fig. 7**). Re-analysis of a published dataset from a model using a different IAV strain (H3N2) and histologically normal lung tissue (Matos 2019) revealed a pronounced induction of *ACOD1* and *TNFAIP3* expression, but (as opposed to *in vivo* infection of mouse lung) not induction of *HMOX1* or *2* (**Fig. S9).**

Anti-inflammatory effects of itaconate, DI, and 4OI on IAV-infected PBMC. PBMC play important roles in influenza infection as they contain cells of innate and adaptive immunity, and because circulating monocytes (which can sustain a nonproductive influenza virus infection) are considered an important source of cytokines that support systemic spread of inflammation (Duan, Hibbs et al., 2016). We therefore investigated effects of the compounds on IAV infected PBMCs both at the bulk and single cell levels. Analysis with targeted PCR- and immuno-assays demonstrated vigorous transcription of viral RNA, induction of *ACOD1* mRNA, and a brisk pro-inflammatory response both at the mRNA and protein level (**Fig. 8A,B**). The induction of *ACOD1* mRNA expression in peripheral blood in IAV infection was also corroborated by reanalysis of a published dataset from whole blood from patients with moderate and severe influenza (**Fig. S10**). The effects of itaconate were mixed in that there was no significant change in *ACOD1*, *IFNB1*, and *TNF* mRNA expression in cells or of IL1B protein in supernatants. In contrast, DI and 4OI led to a marked reduction of IFN and pro-inflammatory cytokine expression at the mRNA and protein level, as well as of *ACOD1* mRNA. As exemplified by the effect of DI

and 4OI on *TNF* and *ACOD1* expression, the treatments reduced expression of some mRNA targets even in uninfected cells, suggesting that they also reduced some baseline inflammation. Of note, 4OI in addition led to a pronounced (95%) reduction in *HA* transcription (p=<0.0001), indicating inhibition of viral RNA replication. PCA of bulk PBMC transcriptomes revealed strong effects of the compounds on cell transcriptomes in general, which led to one outlying DI-treated sample and two itaconate-treated samples, whereas all four 4OI-treated samples formed a clearly discernible group (**Fig. S11**). The most significant transcriptome changes were driven by 4OI, which had major effects on many genes that were not regulated by IAV infection or itaconate or DI treatments (**EV4**). Nonetheless, induction of *HMOX1* by DI in IAV-infected samples was evident. Functional enrichment analysis of GO terms based on the transcriptomes revealed that infection induced the expected antiviral responses, including *response to IFN-I*, as well as several other inflammation-related terms (**Fig. 8C**). At least one of the three compounds prevented activation of each of the infection-associated terms. However, consistent with its lack of effect on *IFNB* expression (**Fig. 8**), itaconate did not affect *response to IFN-I* or *influenza A*. Several terms that were depleted by the compounds in infected PBMC were not enriched by infection alone, suggesting that the compounds diminished also a baseline activation of the PBMC. Interestingly, 4OI treatment strongly enriched terms relating to chromatin conformation, which turned out to be driven by upregulation of histone deacetylase epression. A KEGG pathway analysis essentially confirmed the findings of the GO term analysis (**Fig. S12**), including that 4OI enriched pathways relating to chromatin structure such as *Alcoholism*. Taken together, these results consolidated our above findings that itaconate and derivatives can modulate inflammation due to IAV infection, but also suggested that DI and 4OI may have more robust anti-IFN and anti-inflammatory effects than itaconate. Considering the variable anti-inflammatory effects of itaconate and the miscellaneous effects of 4OI on gene expression in this model, we subsequently focused on DI to decipher effects at the single-cell level.

Single-cell RNAseq of PBMC identifies monocytes as the main PBMC host cell of IAV infection, sole source of *ACOD1* expression, and predominant target of immunosuppressive effects. Thirteen cell types could be identified in the PBMC scRNAseq data set, but we focused the analyses on the overarching five cell types: CD4+ and CD8+ T cells, B cells, NK cells, and monocytes (**Fig. 9A,B**). Monocytes constituted the least numerous cell type, and DI treatment of

control and infected cells led to a further reduction (**Fig. S13**). It was not possible to discern whether this was due to decreased survival or a technical artefact. Monocytes were essentially the only cell type expressing viral RNA, as only negligible amounts of viral transcripts were detected in lymphocytes and NK cells. DI treatment appeared to result in a slight increase in viral RNA expression in monocytes (**Fig. 9C**). IAV infection upregulated expression of *ACOD1* exclusively, and *CXCL10* predominantly, in monocytes, whereas *TNFAIP3*, *IFIT1*, and *ISG15* were upregulated also in the NK, T and B cell compartments (**Fig. 9D**). DI treatment markedly reduced expression of *ACOD1*, *IFIT1*, and *CXCL10*, but –interestingly– it reduced *TNFAIP3* and *ISG15* (albeit weakly) expression only in monocytes. Consistent with the observation that they constituted the main PBMC host cell, IAV infection triggered the most vigorous transcriptomic host response in monocytes, which was driven by the expected IFN responses (**Fig. 9E**). However, discernable differential expression (mostly of IFN-related RNAs) was also observed in the other cell types. CD8+ T cells are shown as a representative example in **Fig. 9F**, the other cell types in **Fig. S14**. Monocytes were the only cell type that mounted a transcriptomic response to DI treatment of uninfected cells. In infection, treatment with DI led to a global downregulation of IFN-related transcripts in monocytes and also downregulation of a subpopulation of IFN-related transcripts in lymphocytes and NK cells. When considering all DEGs irrespective of magnitude of differential expression, DI exerted comparable effects on monocytes and T cells, and only somewhat less on B cells. However, when considering only transcripts with FC >|2|, a preferential effect on monocytes became apparent (**Fig. 9G,H**).

GO term enrichment analysis of the monocyte scRNAseq data confirmed the major enrichment of IFN-related processes by infection and their depletion by DI treatment, which had been seen in all models in this study. In addition, infection broadly dampened RNA metabolism, ribosome assembly, and protein synthesis and export, which was consistent with the cytostatic effects of type I IFN. DI treatment reversed all these effects and also stimulated some in uninfected cells (**Fig. 10A**). A KEGG enrichment analysis of these monocyte data confirmed the depletion of IFN-related pathways (*influenza, measles, cytosolic DNA sensing pathway*) by DI treatment, but also of other pro-inflammatory pathways (*TLR signaling, cytokine-cytokine receptor interaction, NF-kB signaling*) in infected and uninfected cells (**EV5).** Of note, DI treatment apparently stimulated ribosome function in both infected and control monocytes.

The Venn diagrams in **Fig. 10B** illustrate that monocytes are the cell type in which the most biological processes were activated by infection and depleted by DI treatment, but reduction of antiviral and pro-inflammatory responses was a common theme in the other cell types as well (**Fig. 10C**). Indeed, GO term analysis identified four major IFN-related processes as a central functional network that was upregulated by infection and downregulated by DI treatment during infection in all five cell types (**Fig. 10B**). A marked stimulation of protein synthesis and export by DI was also apparent in the uninfected lymphocytes and NK cells. Finally, in order to identify a common transcriptomic network we performed GO and KEGG pathway enrichment analyses of the 81 transcripts that were commonly differentially expressed in IAV infection and regulated in the opposite direction by DI treatment in all five cell types (center of the Venn diagram in **Fig. 9G**). While the GO analysis by and large confirmed the findings shown in **Fig. 10B,** the KEGG pathway analysis revealed a major effect of DI treatment on *allograft rejection*, *graft-vs.-host disease*, and *antigen processing and presentation*, suggesting a broader interference with immune cell activation by DI (**Fig. S15**).

Discussion

In this first dedicated study on the impact of itaconate and derivatives on host responses to IAV infection, we found that (i) the endogenous ACOD1/itaconate axis limits infection-induced pulmonary inflammation in a murine model, (ii) ectopically expressed ACOD1 possesses anti-IFN activity in an epithelial cell line that normally does not express this enzyme, and (iii) that exogenously applied itaconate and/or derivatives restrict IFN-responses and modulate classic pro-inflammatory cytokines across all models tested.

Anti-inflammatory effects of itaconate and derivatives. A major suppression of IFN and some pro-inflammatory cytokine responses was the recurrent theme in all models, i.e. immortalized cells, primary cells, and human lung tissue. This is fully consistent with the early reports that DI has strong anti-inflammatory properties (Lampropoulou 2016), which was subsequently corroborated in diverse models of inflammation and infection, also using 4OI (e.g., (Gu 2020, Xu, Jiang 2020a, Zhao 2019). We used itaconate and DI in parallel in several models, which enabled comparing their relative effectiveness. Overall, results with DI were most consistent, and in spite of its higher toxicity on A549 cells than on dTHP-1 cells, the lower dose still possessed strong anti-inflammatory effects. Itaconate effects were less consistent and much higher doses had to be used to achieve anti-IFN effects similar to DI. Itaconate did not reduce expression of *IFNB1*, *TNF* mRNA or IL1B protein in PBMC. The lack of *TFN* repression by itaconate in that model is consistent with previous reports that it usually does not affect TNF-α levels (Bambouskova et al., 2018). Recent work has also revealed the potential of itaconate to actually enhance IL1B release (Muri 2020). Of note, at higher doses, itaconate and strong electrophilic compounds can actually increase inflammation due to CASP-8 dependent inflammasome activation, and this effect is magnified when the cells are not pre-incubated with the compound before adding the pro-inflammatory stimulus (Muri 2020), as we did in PBMC infections. However, these authors did not investigate effects on IFN suppression. 4OI demonstrated the expected potent anti-inflammatory effects, but also broad effects on processes relating to, e.g., chromatin structure, the potential effects of which on cell homeostasis and cell-pathogen interactions will require further study.

Anti-inflammatory effect of ectopic synthesis of itaconate in A549 cells. Despite the multitude of studies on effects of exogenous administration of itaconate derivatives on cellular inflammation, it had not been tested whether ectopic synthesis of itaconate in a cell type that does not naturally express *ACOD1* has similar effects. Our transfection study (Fig. 5) demonstrated that ectopic, endogenously synthesized itaconate exerts very similar anti-IFN effects as exogenously added itaconate or DI. Of note, the achieved itaconate concentration is very close to that measured in LPS/IFNγ stimulated dTHP-1 cells (Chen et al, unpublished data), suggesting that it is physiological.

Cell-type specific and -independent anti-inflammatory effects of IA and DI. A particular strength of our study lies in the use of scRNAseq to identify major target cells in peripheral blood. Firstly, this analysis identified monocytes as the major PBMC type that is infected by IAV. Secondly, we found that on one hand DI can attenuate IFN-responses in lymphocytes and NK cell as well, but that the immunosuppressive effect is greatest on monocytes. Taken together, these results suggest that even though pharmacological use of itaconate and derivatives would modulate host responses in a diverse array of cells, monocytes/macrophages likely constitute a major functional hub in the genesis of inflammation in IAV infection and subsequent treatment responses to itaconate-based adjunct treatments.

Antiviral effect of 4OI. Olagnier et al. (2020) recently reported that Nrf2 activators including 4OI and dimethyl fumarate limit inflammation in cellular models of SARS-CoV-2 infection in an NRF2-dependent manner. Of note, as opposed to influenza viruses, infection with SARS-CoV-2 suppresses the NRF2 pathway, which can be reversed in part by treatment with Nrf2 activators. These authors in addition observed an antiviral effect of 4OI, which proved to be independent of NRF2- and type I IFN-signaling. Our finding of a remarkable suppression of IAV RNA expression in PBMC corroborates the notion that 4OI has strong antiviral effects in addition to its well-documented anti-inflammatory properties. Further research is needed to validate our finding in other cell types, as we tested it in PBMC only. Nonetheless, the gene expression analysis of itaconate, DI- and 4OI-infected PBMC identified several processes/pathways uniquely regulated by 4OI. Further research should focus on assessing whether any of them could contribute to the antiviral effect of 4OI.

Infection-independent effects on target cells. By using relatively high doses of itaconate and DI and assessing effects of the compounds on uninfected cells or their effects on processes that were not changed during infection, our study also provides a first comprehensive look at global effects of the compounds on specific target cells. In particular, itaconate and 4OI exerted pronounced effects on gene expression in A549 cells and PBMCs, respectively. Clearly, it will be of great interest to investigate how these effects relate to differences in toxicities on different cell types, or to differences in their effects upon virus-host interactions.

Importance of endogenous ACOD1 expression. In the mouse model, we observed a more severe clinical phenotype and higher inflammation in *Acod1*$^{-/-}$ mice. This agrees with work in a mouse model of *M. tuberculosis* infection, where inflammation and mortality were higher in the *Acod1*$^{-/-}$ animals (Nair 2018). However, IAV infection was also assessed in that study, and deleting the *Acod1* gene did not affect weight loss or survival. Those authors used equal numbers of male and female mice, whereas we used female mice only. Further research is required into possible sex-specific effects of the *Acod1* gene in influenza infection. Of note, we found upregulation of *ACOD1* by IAV infection and its prevention by DI treatment in myeloid cells, i.e. dTHP-1 and peripheral blood monocytes, and upregulation of *ACOD1* mRNA in blood from patients with moderate and severe influenza infection as compared with healthy donors. Thus, induction of *ACOD1* expression (and thereby itaconate synthesis) likely is a common feature in human influenza. We have recently identified the active center of ACOD1 enzyme and found that naturally occurring loss-of-function mutations are extremely rare, suggesting that physiologic itaconate responses have been important in human evolution (Chen 2019). It is therefore tempting to speculate that one beneficial role of an active ACOD1/itaconate axis is to reduce the risk of death or organ damage from infection-associated hyper-inflammation and that loss-of-function genotypes have been selected against during times of high infectious disease burdens.

Clinical implications. The current COVID-19 pandemic has, once again, focused the research limelight on the deleterious effects of overshooting innate immune responses in acute viral infections. In a current report, Lee et al. found that intense IFN responses in PBMC from patients are a hallmark of both severe COVID-19 and influenza (Lee 2020). Of note, a recent systematic review of 45 studies on corticosteroid use for COVID-19 found a significant beneficial effect

(van Paassen 2020), whereas to date there are no clinically effective antivirals against SARS-CoV-2. Therefore, the concept of adjunct treatments to control deleterious host immune responses in viral infections is more pertinent than ever. Considering (i) the well documented cytoprotective properties of itaconate and derivatives and (ii) our findings of remarkable anti-inflammatory and anti-IFN effects in the absence of increased viral replication, itaconate derivatives would constitute a highly promising class of compounds for such applications. Considering the more reliable results obtained with DI as compared to unmodified itaconate, the lower required concentrations of DI and 4OI, but also the striking anti-viral effects of 4OI, it appears that chemical variants of itaconate, rather than its native form, will take the lead in further translational development to the bedside.

Detailed methods are found in the Appendix

Acknowledgements. We thank V. Kaever, H. Bähre and staff of the RCU Metabolomics at Hannover Medical School for support with the itaconate measurements, Elena Reinhard for assistance with the animal experiments, the HZI Animal Facility for expert animal care, the HZI Genome Analytics Platform for microarray and RNA sequencing, L. Gröbe for cell sorting, D. Jonigk and P. Braubach (Institute of Pathology, Hannover Medical School) for providing human lung tissue. We thank Hans Jörg Hauser (HZI) for helpful comments on the manuscript.

Conflict of interest. The authors declare that none of them have a conflict of interest relating to conduct of the study or publication of the manuscript.

Data Availability

The gene expression data are available through GEO at accession number GSE162210, GSE162260, GSE162261 and GSE164922. These data are currently private and access can be given to reviewers. The data previously published in (Wilk et al., 2015) are available at GSE66040.

The Paper Explained

PROBLEM. Interferon responses are part of the primary host defenses against infections. However, excessive inflammation is often a major factor in severe disease or even death due to respiratory infections such as influenza, as it can lead to acute respiratory distress syndrome and sepsis-like multiorgan involvement.

RESULTS. We applied itaconate and derivatives to influenza A virus infected human cells and lung tissue and found that these compounds markedly repress interferon responses and some pro-inflammatory processes without increasing viral replication. In fact, 4-octyl itaconate greatly decreased viral RNA replication in peripheral blood mononuclear cells. Single cell RNA sequencing identified monocytes as the predominant blood cell infected with the virus and also the major target of itaconate activity.

IMPACT. The results suggest that novel medications based on itaconate may be effective in dampening deleterious inflammation in influenza infection without the risk of favoring viral spread in the patient.

Figure legends

Figure 1. Reciprocal interactions between *Acod1* expression and inflammation during influenza A virus infection in mice. A. Higher pulmonary expression of *Acod1, Tnfaip3,* and *Hmox1* and *2* mRNA in DBA/2J (D2) than in C57BL/6J (B6) mice following IAV infection (reanalysis of published RNAseq data (Wilk et al., 2015)) (n=3 each strain and time point). *p<0.05; **p<0.01; ***p<0.001 (pairwise t-test with Bonferroni-Holm multiple comparisons correction). **B.** *Acod1* mRNA is among the most highly upregulated transcripts in mouse lung within 48 h of IAV infection (RNAseq, n=8 per time point). **C.** Lower pulmonary levels of itaconate in IAV-infected *Acod1*$^{+/-}$ than in *Acod1*$^{+/+}$ mice. Itaconate was not detected in the *Acod1*$^{-/-}$ mice. (n=36 *Acod1*$^{+/+}$, 27 *Acod1*$^{+/-}$, 4 *Acod1*$^{-/-}$ mice). *p<0.05; **p<0.01; ***p<0.001 (unpaired t-test). **D.** Greater weight loss of female *Acod1*$^{-/-}$ C57BL/6J mice during infection with IAV. Mice had to be euthanized when weight loss exceeded 20%; n=9 *Acod1*$^{+/+}$, 10 *Acod1*$^{+/-}$, 9 *Acod1*$^{-/-}$ mice. *p<0.05; **p<0.01; ***p<0.001 (unpaired t-test) **E.** Survival data of the same experiment as in C. Median survival after day 7 was significantly lower in *Acod1*$^{-/-}$ mice (p=0.018, Mann-Whitney-U test). **F.** Semi-quantitative histopathological scoring of lungs on days 8/9 (mid), 11 and 14 (late) reveals highest inflammation in *Acod1*$^{-/-}$ mice; n=9 *Acod1*$^{+/+}$, 10 *Acod1*$^{+/-}$, 9 *Acod1*$^{-/-}$ mice (all female). *p<0.05; **p<0.01; ***p<0.001 (two-way ANOVA, Tukey's multiple comparisons test) **G.** H&E stained lung sections showing inflammation severity scores of 0 (left) and 3 (right).

Figure 2. Differences among human myeloid cells in *ACOD1* mRNA induction during IAV infection. A. Induction of *ACOD1* and *TNFAIP3* mRNA (RT-qPCR) in M1 and M2 macrophages and PBMCs during IAV infection. **B.** Induction of *ACOD1* and *TNFAIP3* (RT-qPCR) in dTHP-1 cells correlates with virulence of three IAV strains. Mean ±SEM (n=4). *HA* = IAV hemagglutinin. *p<0.05; **p<0.01; ***p<0.001 (two-way ANOVA, Tukey's multiple comparisons test, with reference to M1 macrophages in A, and to Gi-WT in B).

Figure 3. Effects of itaconate and DI on cellular inflammation due to IAV infection of dTHP-1 cells. A. Outline of experiment. dTHP-1 cells were treated with itaconate or DI overnight, or left untreated, and then infected with IAV. Dose-response curves of effects of a range of itaconate and DI and concentrations on *HA* and *CXCL10* mRNA expression are shown

in **Fig. S1. B-C**. 48 h time course, DI = 0.25 mM (n=3). mRNA expression (RT-qPCR) of *HA* (**B**) and *CXCL10* mRNA (**C**) *p<0.05; **p<0.01; ***p<0.001 (unpaired t-test). **D-I.** Global transcriptomic changes (microarray analysis) due to itaconate (25 mM) and DI (1 mM) treatment of uninfected and IAV-infected dTHP-1 cells (n=4). **D.** Venn diagram showing unique and common differentially expressed genes by itaconate and DI treatment of infected cells. **E-I.** Volcano plots showing differential mRNA expression in uninfected dTHP-1 cells under itaconate and DI treatment (**E-F**) and infected dTHP-1 cells with or without itaconate or DI treatment (**G-I**). **J.** Effects of itaconate (25 mM) and DI (1 mM) treatment on levels of inflammation-related polypeptides in dTHP-1 cell supernatants 12 h after IAV infection or mock infection. Mean ± SEM (n = 3). *p<0.05; **p<0.01; ***p<0.001 (One-way ANOVA, Tukey's multiple comparison test).

Figure 4. Itaconate and DI treatment leads to a global downregulation of IFN-I signaling in IAV-infected dTHP-1 cells. Enrichment analysis of gene ontology (GO Biological Process) terms based on the microarray data shown in Fig. 3, using DEGs (p<0.05, FC >|1.5|) as input. GO terms (FDR ≤0.05) reveal major induction of antiviral and inflammatory responses by infection, which are decreased by both itaconate and DI treatment.

Figure 5. Effect of overexpression of ACOD1 and exogenous treatment with DI on IAV-infected A549 cells. A. A549 cells were transfected with pCMV6-Hu-ACOD1, pCMV6 empty vector, or mock transfected for 48 h and then infected with IAV for 48 h (n=3). Expression of the indicated mRNAs was measured by RT-qPCR, itaconate concentrations by LC-MS/MS. *p<0.05; **p<0.01; ***p<0.001 (2-way ANOVA, Tukey's multiple comparisons test) **B.** A549 cells were treated with 0.25 mM DI overnight, infected with IAV for 48 h (n=3), and expression of the indicated mRNAs measured by RT-qPCR. Mean ± SEM (n = 3). *p<0.05; **p<0.01; ***p<0.001 (2-way ANOVA, Sidak's multiple comparisons test).

Figure 6. GO term enrichment analysis of itaconate and DI reveals global effects on IFN-signaling and cellular inflammation in A549. A549 cells were, in the case of treatment, incubated overnight with DI (0.5 mM) or itaconate (20 mM), and then infected with strain PR8M. Gene expression was determined by microarray analysis 24 h p.i. (n=3). **A**. GO enrichment (FDR <0.05) analysis using DEGs (p<0.05, FC >|1.5|) as input. **B**. Hierarchical

cluster analysis illustrating itaconate treatment downregulating a subset of genes involved in IFNA/B signaling.

Fig. 7. Anti-inflammatory effect of itaconate and DI on IAV-infected human lung tissue explants. Human primary lung tissue from patients with emphysema and pulmonary arterial hypertension was incubated overnight with itaconate (25 mM), DI (1 mM), or medium only and was then infected with IAV for 24 h (5 donors, 3 tissue pieces per donor). **A**. Viral titers in supernatant (focus forming assay). **B-D**. *CXCL10* mRNA (**B**), and ISG15 (**C**) mRNA in tissue (RT-qPCR); IP10 concentration in supernatant (EIA) (**D**). Mean ± SEM (n=6). *p<0.05; **p<0.01; ***p<0.001 (Mann-Whitney U test).

Fig. 8. Anti-inflammatory effects of DI and 4OI on IAV-infected human PBMCs. PBMCs were isolated from freshly donated human blood and then infected with IAV for 12 h in the presence or absence of itaconate (10 mM), DI (0.5 mM), or 4OI (25 µM) without preincubation (7 donors, 3 replicates). **A.** Expression of the indicated mRNAs in PBMC (RT-qPCR). **B.** Concentrations of the indicated proteins in PBMC supernatants (ELISA). Mean +/- SEM (6 donors, 3 replicates per donor). *p<0.05; ***p<0.01; ***p<0.001 (1-way ANOVA). **C.** GO enrichment analysis of effects of IA, DI, and 4OI on IAV-infected PBMC. Microarray analysis of PBMC RNA from four of the donors featured in **A-B**. RNA was pooled from the three replicates of each donor, resulting in 4 samples per group. GO term analysis was performed on DEGs (p<0.05, FC>|1.5|) and terms with an FDR <0.02 in at least one condition are shown.

Fig. 9. Single-cell transcriptomic responses of PBMC to IAV infection and DI treatment. PBMCs were isolated from freshly donated human blood (one donor), and then infected with IAV for 12 h with or without DI (0.5 mM) in the medium. **A-B**. UMAP plots identifying 13 cell types (**A**) that make up the five major cell types (**B**) studied. The RNA cell markers used are listed in Table S1. **C-D.** Differential mRNA expression in uninfected, infected and infected/DI-treated PBMCs. **E.** Differential mRNA expression in monocytes in the indicated paired comparisons. Major transcriptional reprogramming due to IAV infection is evident, which is largely prevented by treatment with DI. **F.** Differential mRNA expression in CD8+ T cells in the indicated paired comparisons. Reprogramming in the presence of IAV is much less, but a DI treatment effect is evident. **G-H.** Venn diagrams based on RNAs differentially regulated (FDR

<0.05) by both viral infection and DI treatment in each of the 5 major cell type, either irrespective of FC (**G**) or FC >|2| (**H**).

Figure 10. GO enrichment analysis at the single cell level of DI effects on uninfected and IAV-infected PBMC. Analysis based on the scRNAseq data shown in Fig. 9. Go terms that are enriched/depleted in all cell types by infection and DI treatment are marked with a red asterix. **A.** GO enrichment analysis of monocytes. **B.** Venn diagrams illustrating GO terms that are commonly or uniquely regulated (FDR <0.05) in monocytes, CD4 T cells, CD8 T cells, B cells, and NK cells; due to infection alone, DI treatment of infected cells, or DI treatment of uninfected cells. **C**. Go term analysis of CD4 T cells, CD8 T cells, B cells, and NK cells.

EV1 A. Hierarchical clustering analysis of effects of itaconate and DI on IAV-infected dTHP-1 cells. Analysis based on the same microarray data as used for Fig. 3 and EV1B, using the top 100 DEGs (FDR F-test <1.89E-09). Uninfected cells and untreated IAV-infected cells form one clade and itaconate and DI treated IAV-infected cells the other clade. The brackets identify (i) a large pro-inflammatory subclade in IAV infection, which is globally downregulated by the treatments; (ii) a large cluster of DEGs specific for itaconate treatment; (iii) a small cluster of DEGs specific for DI treatment, and (iv) a subclade comprising DEGs differentially expressed due to both compounds. **B. Enrichment plots based on the 99 genes contained in GO term *Response to type I interferon*.** Enrichment scores are plotted on the y-axis, the mRNAs (identified by vertical lines) along the x-axis, ranked by fold change. The plots illustrate pronounced enrichment in a large number of genes due to infection, which is nearly quantitatively depleted by treatment with both itaconate and DI. **C. 4OI prevents increased NFκB nuclear localization in IAV infection.** IAV infection of dTHP-1 cells, with or without treatment with IA (25 mM), DI (0.5 mM) and 4OI (25 μM). Data are based on fluorescent intensities resulting from colocalization of NFκB (red) in nuclei (DAPI, blue) and represent the mean of at least 5 representative images per replicate sample (n=3). *p<0.05; **p<0.01; ***p<0.001 (unpaired t-test with Welch's correction).

EV2. Effects of itaconate (20 mM) and DI (0.5 mM) on transcriptomic responses in IAV-infected A549 cells. Analysis based on the microarray data used for the GO analysis in Fig. 6. Unsupervised hierarchical clustering analysis of the 100 most significant DEGs (FDR F-test

<1.46E-10). DI-treated infected and uninfected cells cluster in one clade, and infected and itaconate-treated infected cells in the other. There is a large clade mostly containing proinflammatory genes, which are downregulated by DI, whereas effects of itaconate are much weaker. *DUSP95* is exclusively downregulated by itaconate (arrowhead). There are two smaller clades of genes that form an "itaconate signature", comprising genes that are, albeit to a lesser extent, also upregulated by IAV infection, or uniquely by itaconate.

EV3. Hierarchical clustering analysis of transcriptomic changes in IAV infected PBMC and responses to itaconate, DI, and 4OI treatment. The 100 most significant DEGs were selected (FDR F-test <3.72E-05). Transcriptome changes are mostly due to marked effects of 4OI (more down- than upregulation) on genes which are not affected by IAV infection, indicating general effects on cell homeostasis. However, induction of *HMOX1* by DI in IAV infection is evident (arrow). The arrow points to the extreme outlier under DI treatment seen in the PCA.

EV4. Cell-type specific KEGG pathway analysis of effects of DI on infected and uninfected monocytes, CD4 T cells, CD8 T cells, B cells, and NK cells. Analyses based on the scRNAseq data used for Fig. 9 and 10.

References

Alberts R, Srivastava B, Wu H, Viegas N, Geffers R, Klawonn F, Novoselova N, do Valle TZ, Panthier JJ, Schughart K (2010) Gene expression changes in the host response between resistant and susceptible inbred mouse strains after influenza A infection. *Microbes Infect* 12: 309-18

Bambouskova M, Gorvel L, Lampropoulou V, Sergushichev A, Loginicheva E, Johnson K, Korenfeld D, Mathyer ME, Kim H, Huang LH, Duncan D, Bregman H, Keskin A, Santeford A, Apte RS, Sehgal R, Johnson B, Amarasinghe GK, Soares MP, Satoh T et al. (2018) Electrophilic properties of itaconate and derivatives regulate the IkappaBzeta-ATF3 inflammatory axis. *Nature* 556: 501-504

Chen F, Lukat P, Iqbal AA, Saile K, Kaever V, van den Heuvel J, Blankenfeldt W, Bussow K, Pessler F (2019) Crystal structure of cis-aconitate decarboxylase reveals the impact of naturally occurring human mutations on itaconate synthesis. *Proc Natl Acad Sci U S A* 116: 20644-20654

Cho H, Proll SC, Szretter KJ, Katze MG, Gale Jr M, Diamond MS (2013) Differential innate immune response programs in neuronal subtypes determine susceptibility to infection in the brain by positive-stranded RNA viruses. *Nature medicine* 19: 458-464

Collaborators GI (2018) Mortality, morbidity, and hospitalisations due to influenza lower respiratory tract infections, 2017: an analysis for the Global Burden of Disease Study 2017. *Lancet Resp Med* 7: 69-89

Cordes T, Lucas A, Divakaruni AS, Murphy AN, Cabrales P, Metallo CM (2020) Itaconate modulates tricarboxylic acid and redox metabolism to mitigate reperfusion injury. *Mol Metab* 32: 122-135

Cordes T, Michelucci A, Hiller K (2015) Itaconic Acid: The Surprising Role of an Industrial Compound as a Mammalian Antimicrobial Metabolite. *Annu Rev Nutr* 35: 451-73

Cordes T, Wallace M, Michelucci A, Divakaruni AS, Sapcariu SC, Sousa C, Koseki H, Cabrales P, Murphy AN, Hiller K, Metallo CM (2016) Immunoresponsive Gene 1 and Itaconate Inhibit Succinate Dehydrogenase to Modulate Intracellular Succinate Levels. *J Biol Chem* 291: 14274-84

Daniels BP, Kofman SB, Smith JR, Norris GT, Snyder AG, Kolb JP, Gao X, Locasale JW, Martinez J, Gale M, Jr., Loo YM, Oberst A (2019) The Nucleotide Sensor ZBP1 and Kinase RIPK3 Induce the Enzyme IRG1 to Promote an Antiviral Metabolic State in Neurons. *Immunity* 50: 64-76 e4

Duan M, Hibbs ML, Chen W (2016) The contributions of lung macrophage and monocyte heterogeneity to influenza pathogenesis. *Immunol Cell Biol* 95: 225-235

Eklund A (2016) beeswarm: The BeeSwarm Plot, an Alternative to Stripchart. *https://CRANR-projectorg/package=beeswarm*

Gu L, Lin J, Wang Q, Li C, Peng X, Fan Y, Lu C, Lin H, Niu Y, Zhu G, Zhao G (2020) Dimethyl itaconate protects against fungal keratitis by activating the Nrf2/HO-1 signaling pathway. *Immunol Cell Biol* 98: 229-241

Hooftman A, O'Neill LAJ (2019) The Immunomodulatory Potential of the Metabolite Itaconate. *Trends Immunol*

Kuhn M (2017) PhD dissertation. Hannover Medical School. Hannover, Germany.

Lampropoulou V, Sergushichev A, Bambouskova M, Nair S, Vincent EE, Loginicheva E, Cervantes-Barragan L, Ma X, Huang SC, Griss T, Weinheimer CJ, Khader S, Randolph GJ, Pearce EJ, Jones RG, Diwan A, Diamond MS, Artyomov MN (2016) Itaconate Links Inhibition of Succinate Dehydrogenase with Macrophage Metabolic Remodeling and Regulation of Inflammation. *Cell Metab* 24: 158-66

Lee JS, Park S, Jeong HW, Ahn JY, Choi SJ, Lee H, Choi B, Nam SK, Sa M, Kwon JS, Jeong SJ, Lee HK, Park SH, Park SH, Choi JY, Kim SH, Jung I, Shin EC (2020) Immunophenotyping of COVID-19 and influenza highlights the role of type I interferons in development of severe COVID-19. *Sci Immunol* 5

Li Y, Zhang P, Wang C, Han C, Meng J, Liu X, Xu S, Li N, Wang Q, Shi X, Cao X (2013) Immune responsive gene 1 (IRG1) promotes endotoxin tolerance by increasing A20 expression in macrophages through reactive oxygen species. *J Biol Chem* 288: 16225-34

Liu H, Feng Y, Xu M, Yang J, Wang Z, Di G (2018) Four-octyl itaconate activates Keap1-Nrf2 signaling to protect neuronal cells from hydrogen peroxide. *Cell Commun Signal* 16: 81

Matos ADR, Wunderlich K, Schloer S, Schughart K, Geffers R, Seders M, Witt M, Christersson A, Wiewrodt R, Wiebe K, Barth P, Hocke A, Hippenstiel S, Honzke K, Dittmer U, Sutter K, Rescher U, Rodionycheva S, Matera N, Ludwig S et al. (2019) Antiviral potential of human IFN-alpha subtypes against influenza A H3N2 infection in human lung explants reveals subtype-specific activities. *Emerg Microbes Infect* 8: 1763-1776

Michelucci A, Cordes T, Ghelfi J, Pailot A, Reiling N, Goldmann O, Binz T, Wegner A, Tallam A, Rausell A (2013) Immune-responsive gene 1 protein links metabolism to immunity by catalyzing itaconic acid production. *Proceedings of the National Academy of Sciences* 110: 7820-7825

Mills EL, Ryan DG, Prag HA, Dikovskaya D, Menon D, Zaslona Z, Jedrychowski MP, Costa ASH, Higgins M, Hams E, Szpyt J, Runtsch MC, King MS, McGouran JF, Fischer R, Kessler BM, McGettrick AF, Hughes MM, Carroll RG, Booty LM et al. (2018) Itaconate is an anti-inflammatory metabolite that activates Nrf2 via alkylation of KEAP1. *Nature* 556: 113-117

Muri J, Wolleb H, Broz P, Carreira EM, Kopf M (2020) Electrophilic Nrf2 activators and itaconate inhibit inflammation at low dose and promote IL-1beta production and inflammatory apoptosis at high dose. *Redox Biol* 36: 101647

Nair S, Huynh JP, Lampropoulou V, Loginicheva E, Esaulova E, Gounder AP, Boon ACM, Schwarzkopf EA, Bradstreet TR, Edelson BT, Artyomov MN, Stallings CL, Diamond MS (2018) Irg1 expression in myeloid cells prevents immunopathology during M. tuberculosis infection. *J Exp Med* 215: 1035-1045

O'Neill LAJ, Artyomov MN (2019) Itaconate: the poster child of metabolic reprogramming in macrophage function. *Nat Rev Immunol*

Olagnier D, Farahani E, Thyrsted J, Blay-Cadanet J, Herengt A, Idorn M, Hait A, Hernaez B, Knudsen A, Iversen MB, Schilling M, Jorgensen SE, Thomsen M, Reinert LS, Lappe M, Hoang HD, Gilchrist VH, Hansen AL, Ottosen R, Nielsen CG et al. (2020) SARS-CoV2-mediated suppression of NRF2-signaling reveals potent antiviral and anti-inflammatory activity of 4-octyl-itaconate and dimethyl fumarate. *Nat Commun* 11: 4938

Petersen H, Mostafa A, Tantawy MA, Iqbal AA, Hoffmann D, Tallam A, Selvakumar B, Pessler F, Beer M, Rautenschlein S (2018a) NS Segment of a 1918 Influenza A Virus-Descendent Enhances Replication of H1N1pdm09 and Virus-Induced Cellular Immune Response in Mammalian and Avian Systems. *Frontiers in Microbiology* 9: 526

Petersen H, Mostafa A, Tantawy MA, Iqbal AA, Hoffmann D, Tallam A, Selvakumar B, Pessler F, Beer M, Rautenschlein S, Pleschka S (2018b) NS Segment of a 1918 Influenza A Virus-Descendent Enhances Replication of H1N1pdm09 and Virus-Induced Cellular Immune Response in Mammalian and Avian Systems. *Front Microbiol* 9: 526

Preusse M, Schughart K, Pessler F (2017) Host Genetic Background Strongly Affects Pulmonary microRNA Expression before and during Influenza A Virus Infection. *Front Immunol* 8: 246

Preusse M, Tantawy MA, Klawonn F, Schughart K, Pessler F (2013) Infection- and procedure-dependent effects on pulmonary gene expression in the early phase of influenza A virus infection in mice. *BMC Microbiol* 13: 293

R_Core_Team (2014) R: A language and environment for statistical computing. *R Foundation for Statistical Computing, Vienna, Austria* URL http://www.R-project.org/

Ragab D, Salah Eldin H, Taeimah M, Khattab R, Salem R (2020) The COVID-19 Cytokine Storm; What We Know So Far. *Front Immunol* 11: 1446

Ramos I, Fernandez-Sesma A (2015) Modulating the Innate Immune Response to Influenza A Virus: Potential Therapeutic Use of Anti-Inflammatory Drugs. *Front Immunol* 6: 361

Srivastava B, Blazejewska P, Hessmann M, Bruder D, Geffers R, Mauel S, Gruber AD, Schughart K (2009) Host genetic background strongly influences the response to influenza a virus infections. *PLOS One* 4: e4857

Strelko CL, Lu W, Dufort FJ, Seyfried TN, Chiles TC, Rabinowitz JD, Roberts MF (2011) Itaconic acid is a mammalian metabolite induced during macrophage activation. *J Am Chem Soc* 133: 16386-16389

Tang C, Wang X, Xie Y, Cai X, Yu N, Hu Y, Zheng Z (2018) 4-Octyl Itaconate Activates Nrf2 Signaling to Inhibit Pro-Inflammatory Cytokine Production in Peripheral Blood Mononuclear Cells of Systemic Lupus Erythematosus Patients. *Cell Physiol Biochem* 51: 979-990

Uddin MJ, Joe Y, Kim S-K, Jeong SO, Ryter SW, Pae H-O, Chung HT (2016) IRG1 induced by heme oxygenase-1/carbon monoxide inhibits LPS-mediated sepsis and pro-inflammatory cytokine production. *Cellular and Molecular Immunology* 13: 170

van Paassen J, Vos JS, Hoekstra EM, Neumann KMI, Boot PC, Arbous SM (2020) Corticosteroid use in COVID-19 patients: a systematic review and meta-analysis on clinical outcomes. *Crit Care* 24: 696

Wilk E, Pandey AK, Leist SR, Hatesuer B, Preusse M, Pommerenke C, Wang J, Schughart K (2015) RNAseq expression analysis of resistant and susceptible mice after influenza A virus infection identifies novel genes associated with virus replication and important for host resistance to infection. *BMC Genomics* 16: 655

Xu M, Jiang P, Sun H, Yuan X, Gao S, Guo J, Zhao C, Hu X, Liu X, Fu Y (2020a) Dimethyl itaconate protects against lipopolysaccharide-induced endometritis by inhibition of TLR4/NF-kappaB and activation of Nrf2/HO-1 signaling pathway in mice. *Iran J Basic Med Sci* 23: 1239-1244

Xu M, Jiang P, Sun H, Yuan X, Gao S, Guo J, Zhao J, Hu X, Liu X, Fu Y (2020b) Dimethyl itaconate protects against lipopolysaccharide-induced endometritis by inhibition of TLR4/NF-κB and activation of Nrf2/HO-1 signaling pathway in mice. *Iran J Basic Med Sci* 23: 1239-1244

Zhao C, Jiang P, He Z, Yuan X, Guo J, Li Y, Hu X, Cao Y, Fu Y, Zhang N (2019) Dimethyl itaconate protects against lippolysacchride-induced mastitis in mice by activating MAPKs and Nrf2 and inhibiting NF-kappaB signaling pathways. *Microb Pathog* 133: 103541

Figure 1

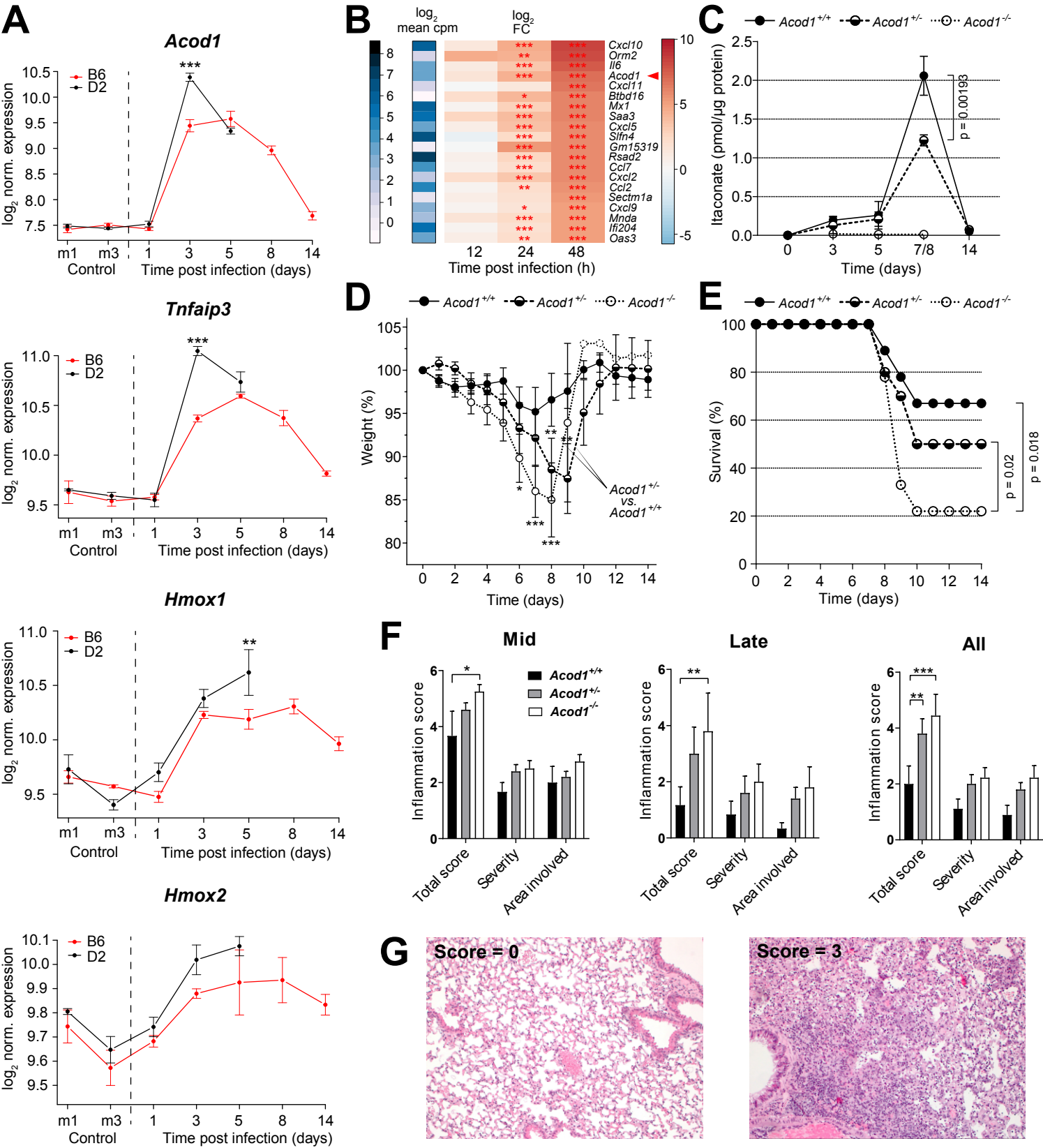
A
Acod1
Tnfaip3
Hmox1
Hmox2
B6
D2
log2 norm. expression
m1
m3
Control
Time post infection (days)
B
log2 mean cpm
log2 FC
Cxcl10
Orm2
Il6
Acod1
Cxcl11
Btbd16
Mx1
Saa3
Cxcl5
Slfn4
Gm15319
Rsad2
Ccl7
Cxcl2
Ccl2
Sectm1a
Cxcl9
Mnda
Ifi204
Oas3
12
24
48
Time post infection (h)
C
Acod1+/+
Acod1+/-
Acod1-/-
Itaconate (pmol/µg protein)
p = 0.00193
Time (days)
D
Weight (%)
Acod1+/- vs. Acod1+/+
Time (days)
E
Survival (%)
p = 0.02
p = 0.018
Time (days)
F
Mid
Late
All
Inflammation score
Total score
Severity
Area involved
G
Score = 0
Score = 3

Figure 2

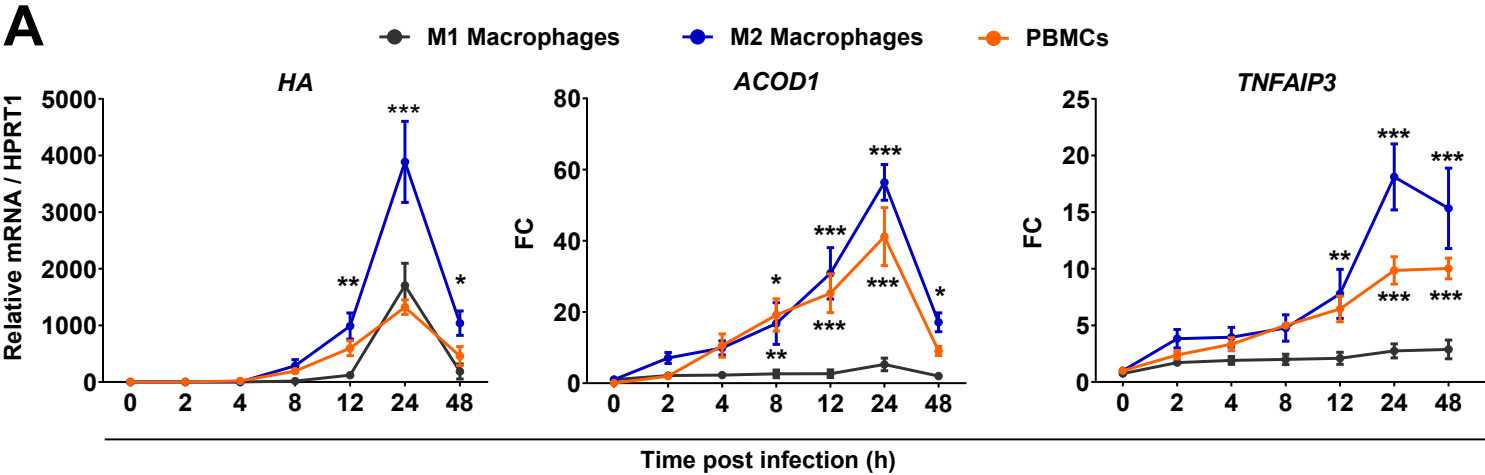
A
M1 Macrophages
M2 Macrophages
PBMCs
HA
ACOD1
TNFAIP3
Relative mRNA / HPRT1
FC
Time post infection (h)

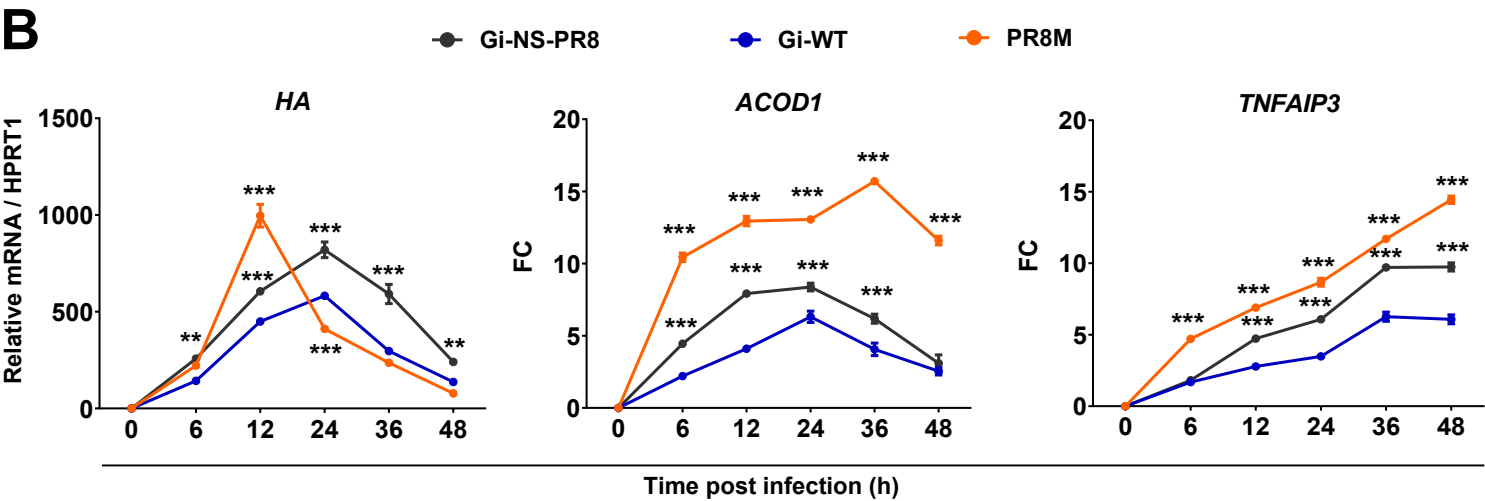
B
Gi-NS-PR8
Gi-WT
PR8M
HA
ACOD1
TNFAIP3
Relative mRNA / HPRT1
FC
Time post infection (h)

Figure 3

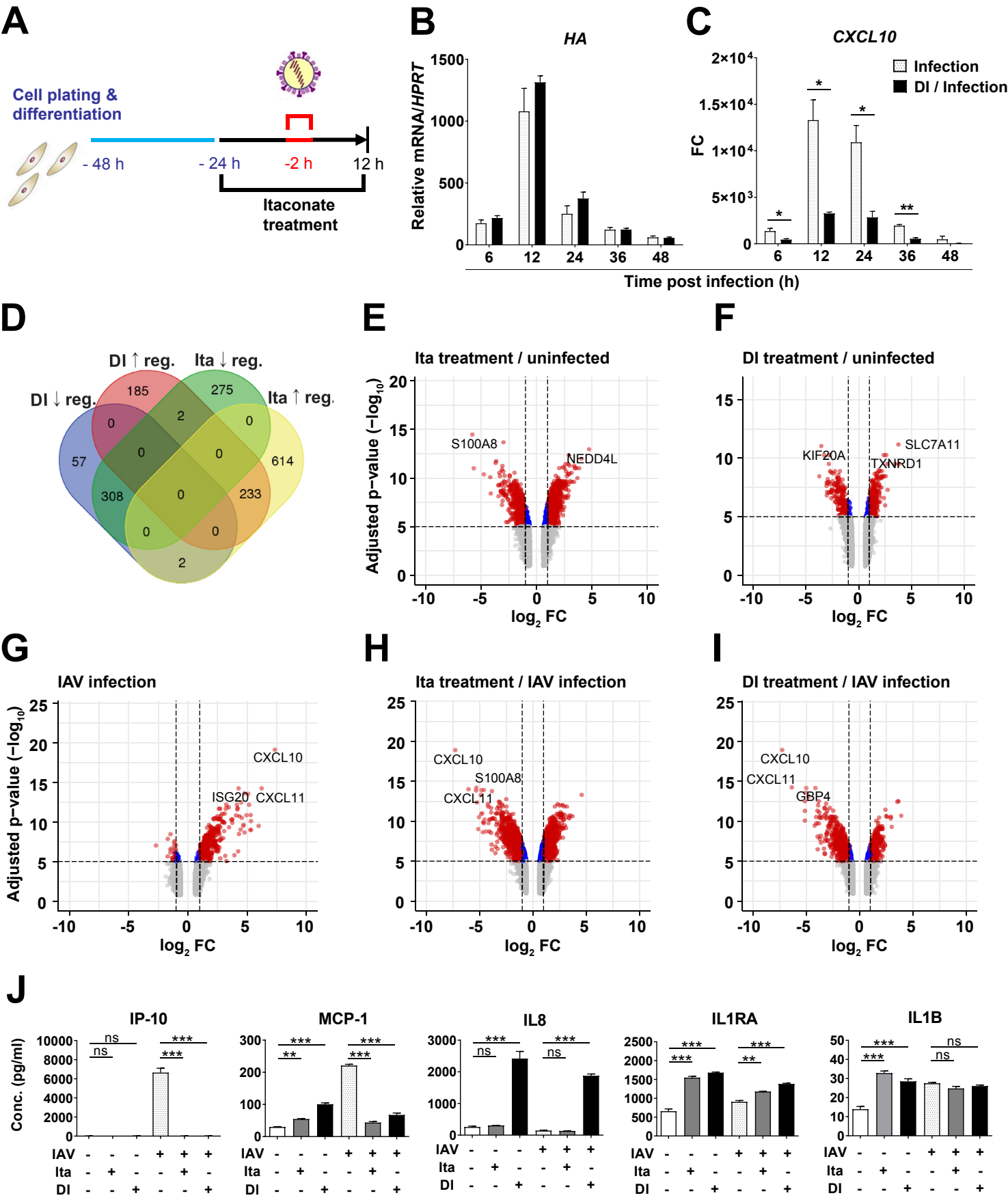
A
Cell plating & differentiation
- 48 h
- 24 h
-2 h
12 h
Itaconate treatment
B
HA
Relative mRNA/HPRT
C
CXCL10
FC
Infection
DI / Infection
Time post infection (h)
D
DI ↑ reg.
Ita ↓ reg.
DI ↓ reg.
Ita ↑ reg.
E
Ita treatment / uninfected
S100A8
NEDD4L
Adjusted p-value (−log10)
log2 FC
F
DI treatment / uninfected
KIF20A
SLC7A11
TXNRD1
G
IAV infection
CXCL10
ISG20
CXCL11
H
Ita treatment / IAV infection
CXCL10
S100A8
CXCL11
I
DI treatment / IAV infection
CXCL10
CXCL11
GBP4
J
IP-10
MCP-1
IL8
IL1RA
IL1B
Conc. (pg/ml)
IAV
Ita
DI

Figure 4

dTHP-1 cells: GO Biological Process (FDR < 0.05)

Figure 5

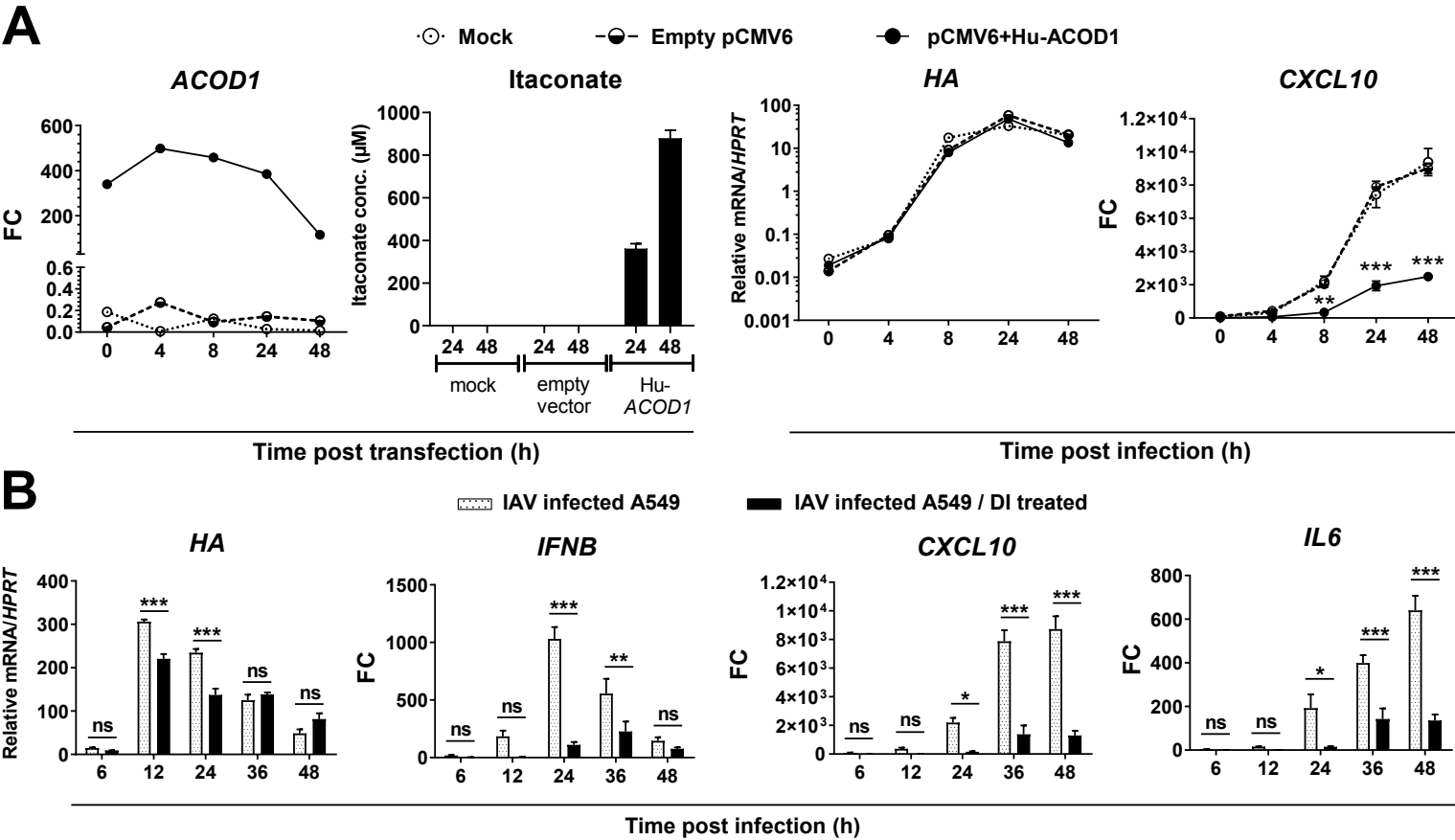
A
Mock
Empty pCMV6
pCMV6+Hu-ACOD1
ACOD1
FC
Itaconate
Itaconate conc. (μM)
24 48 24 48 24 48
mock
empty vector
Hu-ACOD1
HA
Relative mRNA/HPRT
CXCL10
FC
Time post transfection (h)
Time post infection (h)
B
IAV infected A549
IAV infected A549 / DI treated
HA
Relative mRNA/HPRT
IFNB
FC
CXCL10
FC
IL6
FC
ns
Time post infection (h)

Figure 6

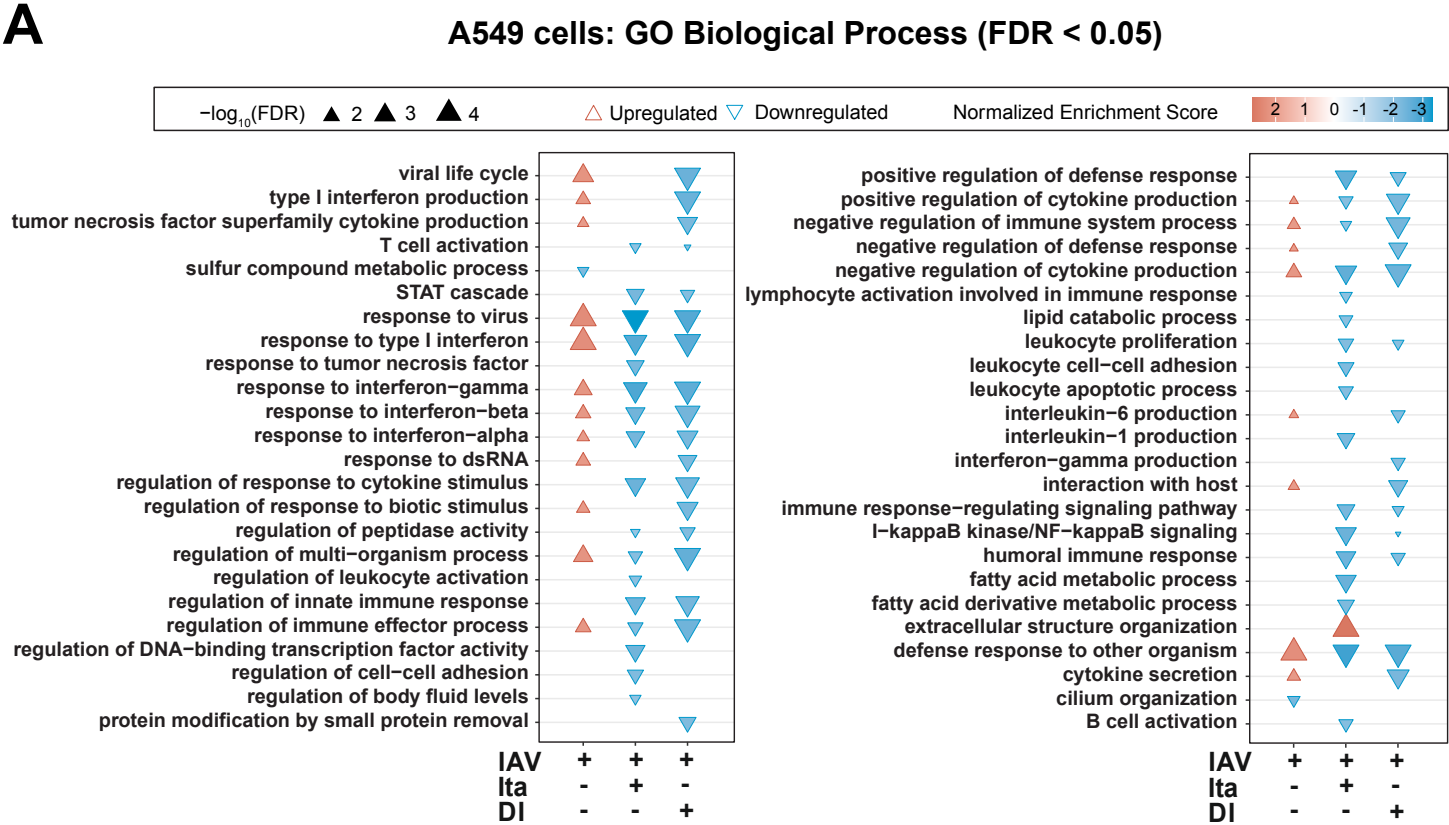
A
A549 cells: GO Biological Process (FDR < 0.05)
−log10(FDR) 2 3 4
Upregulated
Downregulated
Normalized Enrichment Score
2 1 0 -1 -2 -3
viral life cycle
type I interferon production
tumor necrosis factor superfamily cytokine production
T cell activation
sulfur compound metabolic process
STAT cascade
response to virus
response to type I interferon
response to tumor necrosis factor
response to interferon−gamma
response to interferon−beta
response to interferon−alpha
response to dsRNA
regulation of response to cytokine stimulus
regulation of response to biotic stimulus
regulation of peptidase activity
regulation of multi−organism process
regulation of leukocyte activation
regulation of innate immune response
regulation of immune effector process
regulation of DNA−binding transcription factor activity
regulation of cell−cell adhesion
regulation of body fluid levels
protein modification by small protein removal
IAV + + +
Ita - + -
DI - - +
positive regulation of defense response
positive regulation of cytokine production
negative regulation of immune system process
negative regulation of defense response
negative regulation of cytokine production
lymphocyte activation involved in immune response
lipid catabolic process
leukocyte proliferation
leukocyte cell−cell adhesion
leukocyte apoptotic process
interleukin−6 production
interleukin−1 production
interferon−gamma production
interaction with host
immune response−regulating signaling pathway
I−kappaB kinase/NF−kappaB signaling
humoral immune response
fatty acid metabolic process
fatty acid derivative metabolic process
extracellular structure organization
defense response to other organism
cytokine secretion
cilium organization
B cell activation
IAV + + +
Ita - + -
DI - - +

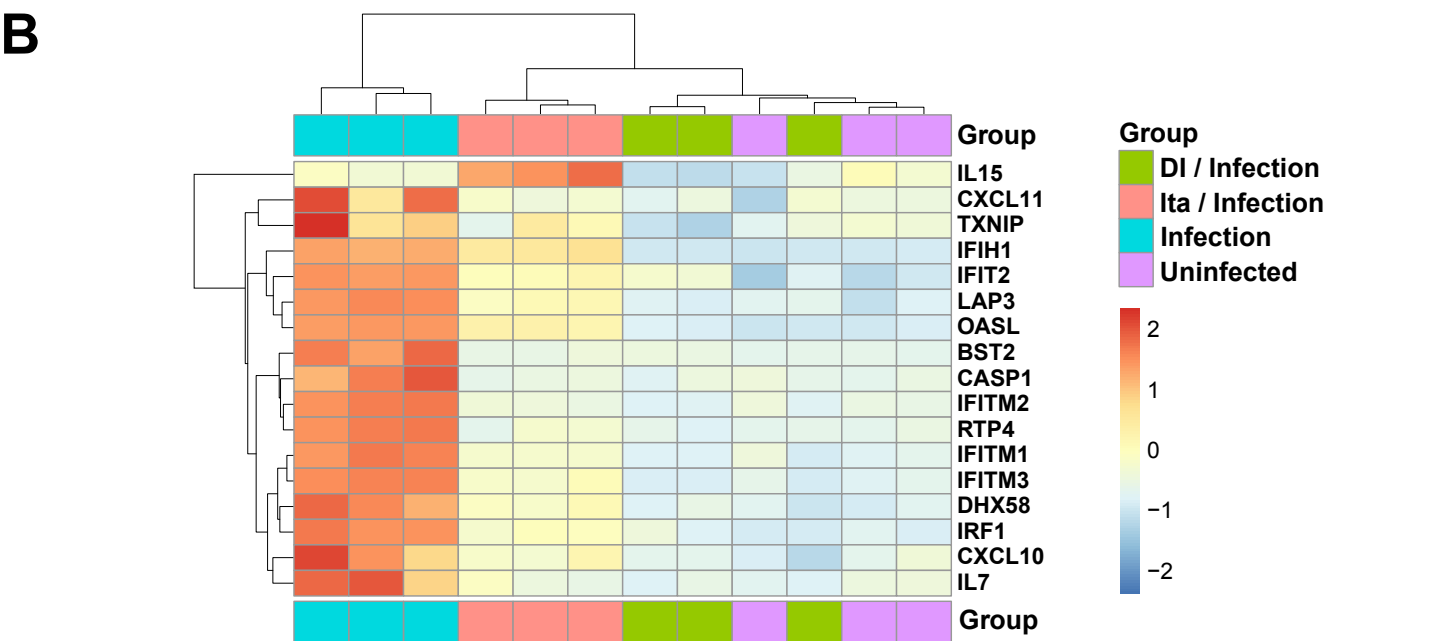
B
Group
IL15
CXCL11
TXNIP
IFIH1
IFIT2
LAP3
OASL
BST2
CASP1
IFITM2
RTP4
IFITM1
IFITM3
DHX58
IRF1
CXCL10
IL7
Group
Group
DI / Infection
Ita / Infection
Infection
Uninfected
2
1
0
−1
−2

Figure 7

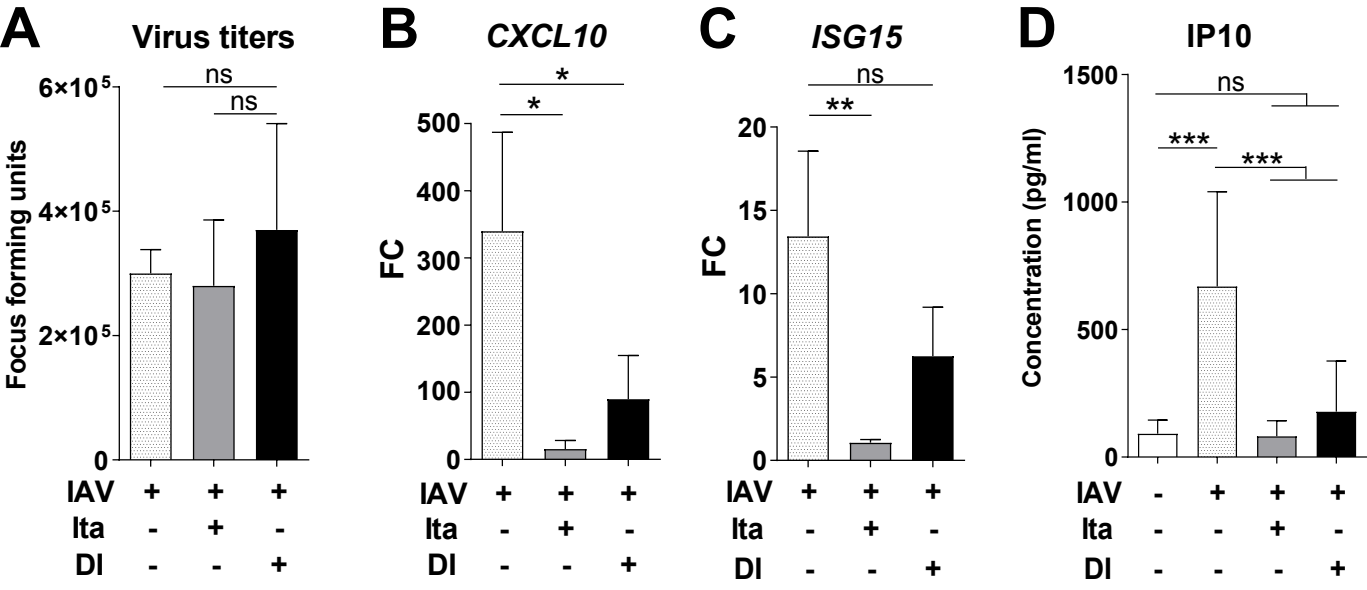
A
Virus titers
Focus forming units
6×10^5
4×10^5
2×10^5
0
ns
ns
IAV + + +
Ita - + -
DI - - +
B
CXCL10
FC
500
400
300
200
100
0
*
*
IAV + + +
Ita - + -
DI - - +
C
ISG15
FC
20
15
10
5
0
ns
**
IAV + + +
Ita - + -
DI - - +
D
IP10
Concentration (pg/ml)
1500
1000
500
0
ns
***
***
IAV - + + +
Ita - - + -
DI - - - +

Figure 8

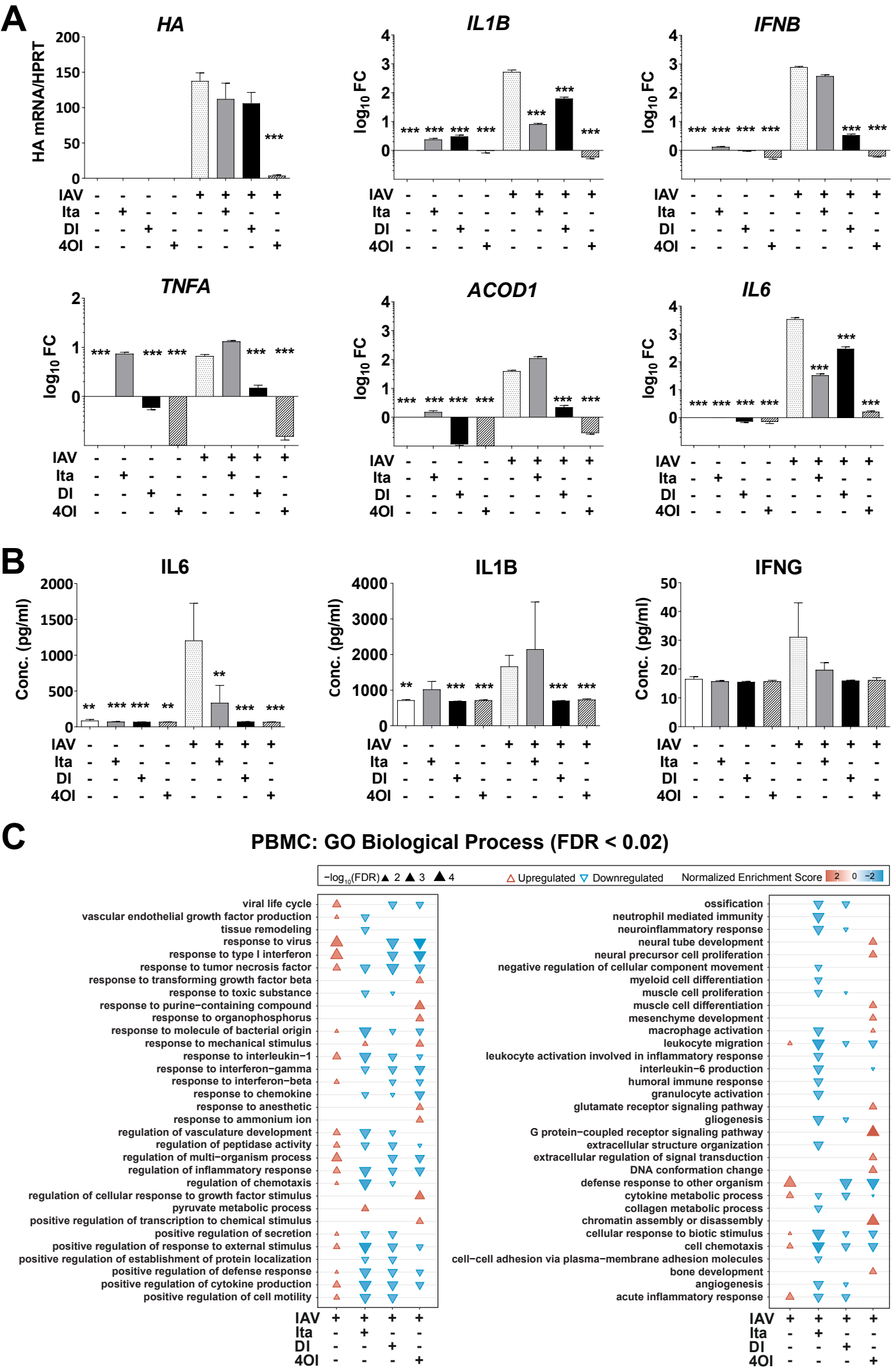
A
HA
HA mRNA/HPRT
IL1B
IFNB
TNFA
ACOD1
IL6
log10 FC
IAV
Ita
DI
4OI
B
IL6
IL1B
IFNG
Conc. (pg/ml)
C
PBMC: GO Biological Process (FDR < 0.02)
−log10(FDR) 2 3 4
Upregulated
Downregulated
Normalized Enrichment Score
viral life cycle
vascular endothelial growth factor production
tissue remodeling
response to virus
response to type I interferon
response to tumor necrosis factor
response to transforming growth factor beta
response to toxic substance
response to purine−containing compound
response to organophosphorus
response to molecule of bacterial origin
response to mechanical stimulus
response to interleukin−1
response to interferon−gamma
response to interferon−beta
response to chemokine
response to anesthetic
response to ammonium ion
regulation of vasculature development
regulation of peptidase activity
regulation of multi−organism process
regulation of inflammatory response
regulation of chemotaxis
regulation of cellular response to growth factor stimulus
pyruvate metabolic process
positive regulation of transcription to chemical stimulus
positive regulation of secretion
positive regulation of response to external stimulus
positive regulation of establishment of protein localization
positive regulation of defense response
positive regulation of cytokine production
positive regulation of cell motility
ossification
neutrophil mediated immunity
neuroinflammatory response
neural tube development
neural precursor cell proliferation
negative regulation of cellular component movement
myeloid cell differentiation
muscle cell proliferation
muscle cell differentiation
mesenchyme development
macrophage activation
leukocyte migration
leukocyte activation involved in inflammatory response
interleukin−6 production
humoral immune response
granulocyte activation
glutamate receptor signaling pathway
gliogenesis
G protein−coupled receptor signaling pathway
extracellular structure organization
extracellular regulation of signal transduction
DNA conformation change
defense response to other organism
cytokine metabolic process
collagen metabolic process
chromatin assembly or disassembly
cellular response to biotic stimulus
cell chemotaxis
cell−cell adhesion via plasma−membrane adhesion molecules
bone development
angiogenesis
acute inflammatory response

Figure 9

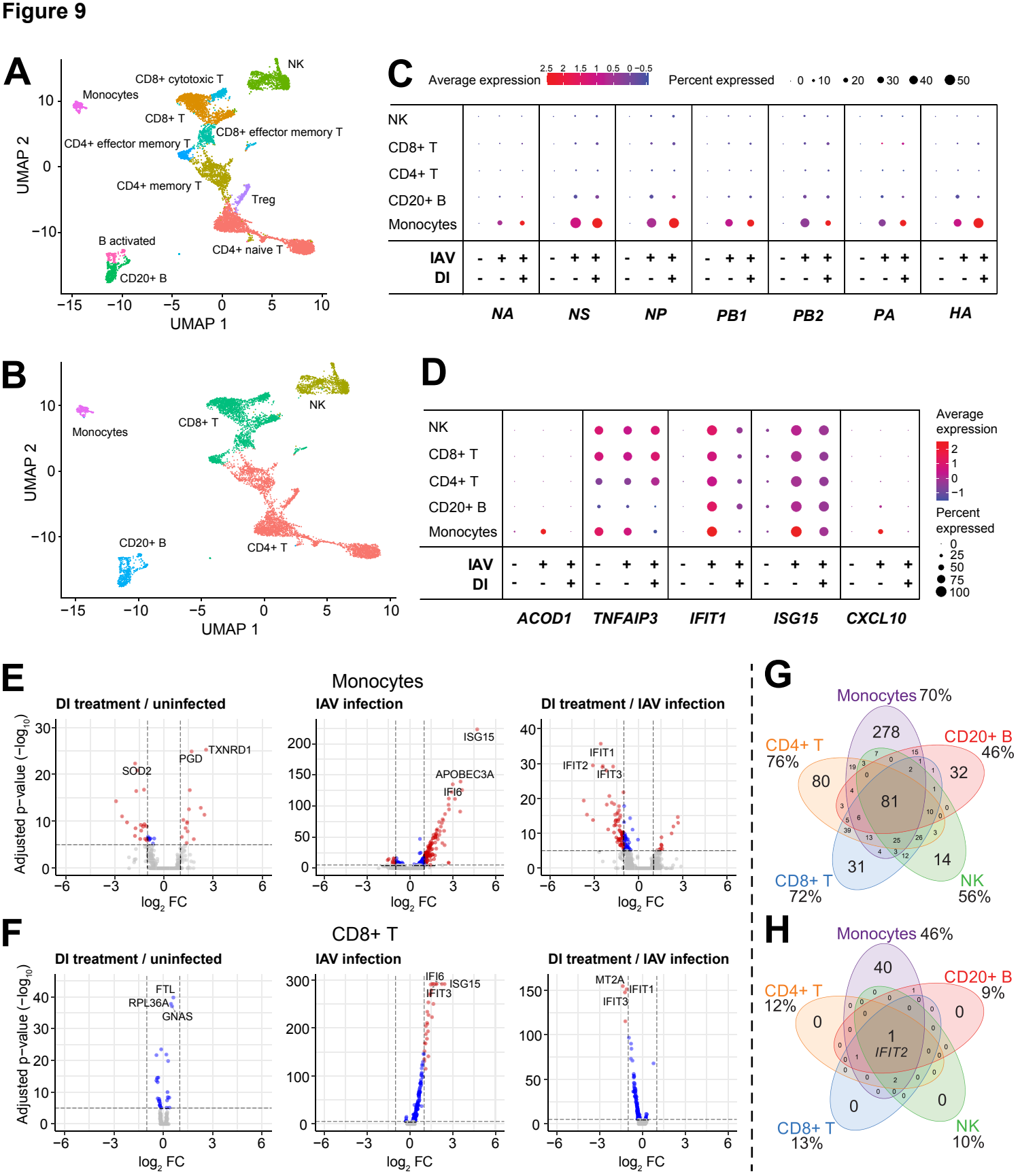
A
NK
CD8+ cytotoxic T
Monocytes
CD8+ T
CD8+ effector memory T
CD4+ effector memory T
CD4+ memory T
Treg
B activated
CD4+ naive T
CD20+ B
UMAP 2
UMAP 1
B
NK
Monocytes
CD8+ T
CD20+ B
CD4+ T
UMAP 2
UMAP 1
C
Average expression
Percent expressed
NK
CD8+ T
CD4+ T
CD20+ B
Monocytes
IAV
DI
NA
NS
NP
PB1
PB2
PA
HA
D
NK
CD8+ T
CD4+ T
CD20+ B
Monocytes
IAV
DI
ACOD1
TNFAIP3
IFIT1
ISG15
CXCL10
Average expression
Percent expressed
E
Monocytes
DI treatment / uninfected
IAV infection
DI treatment / IAV infection
SOD2
PGD
TXNRD1
ISG15
APOBEC3A
IFI6
IFIT1
IFIT2
IFIT3
Adjusted p−value (−log10)
log2 FC
F
CD8+ T
DI treatment / uninfected
IAV infection
DI treatment / IAV infection
FTL
RPL36A
GNAS
IFI6
ISG15
IFIT3
MT2A
IFIT1
IFIT3
Adjusted p−value (−log10)
log2 FC
G
Monocytes 70%
CD4+ T 76%
CD20+ B 46%
CD8+ T 72%
NK 56%
278
80
32
81
31
14
H
Monocytes 46%
CD4+ T 12%
CD20+ B 9%
CD8+ T 13%
NK 10%
40
0
0
1
IFIT2
0
0

Figure 10

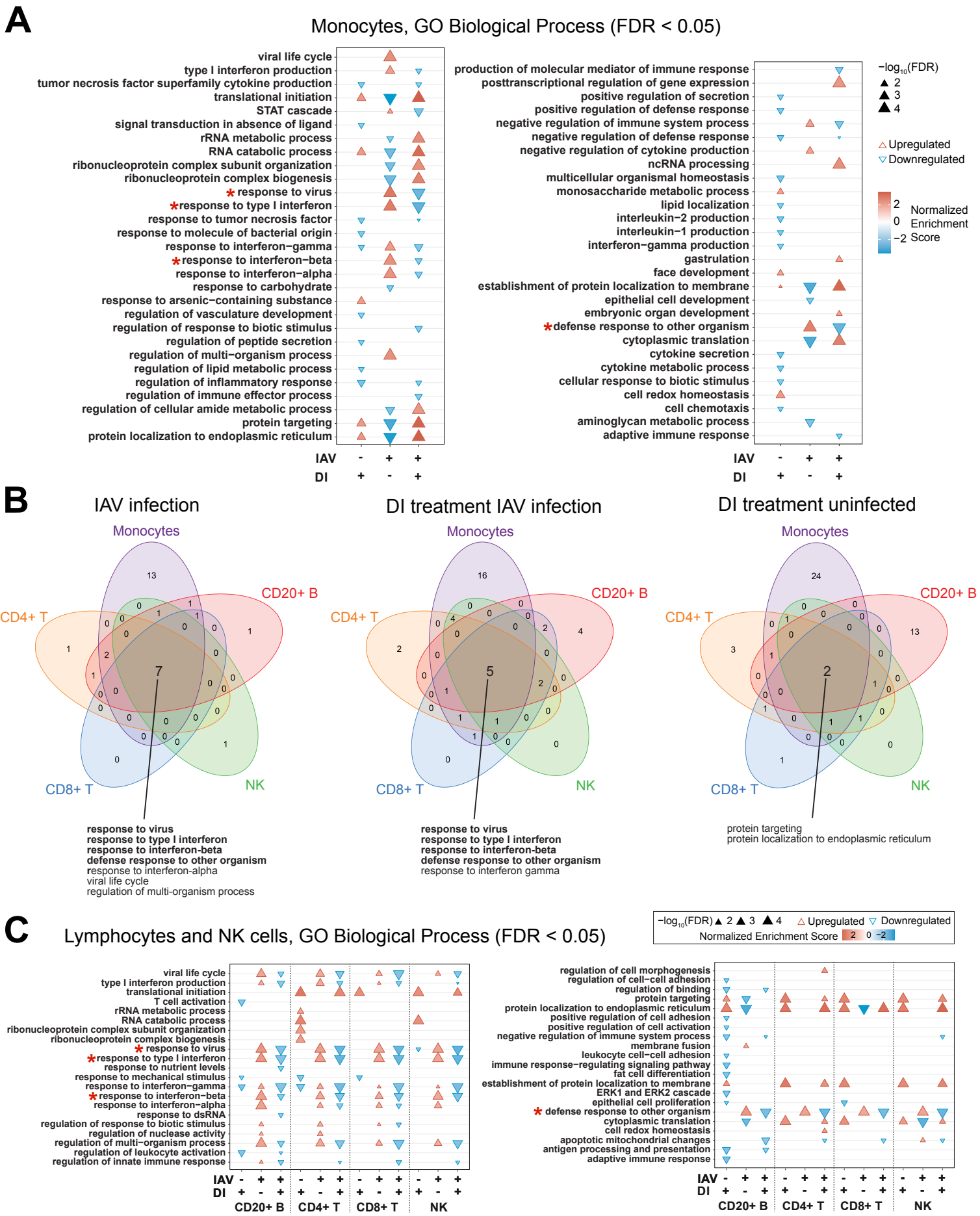
A
Monocytes, GO Biological Process (FDR < 0.05)
viral life cycle
type I interferon production
tumor necrosis factor superfamily cytokine production
translational initiation
STAT cascade
signal transduction in absence of ligand
rRNA metabolic process
RNA catabolic process
ribonucleoprotein complex subunit organization
ribonucleoprotein complex biogenesis
* response to virus
*response to type I interferon
response to tumor necrosis factor
response to molecule of bacterial origin
response to interferon−gamma
*response to interferon−beta
response to interferon−alpha
response to carbohydrate
response to arsenic−containing substance
regulation of vasculature development
regulation of response to biotic stimulus
regulation of peptide secretion
regulation of multi−organism process
regulation of lipid metabolic process
regulation of inflammatory response
regulation of immune effector process
regulation of cellular amide metabolic process
protein targeting
protein localization to endoplasmic reticulum
IAV - + +
DI + - +
production of molecular mediator of immune response
posttranscriptional regulation of gene expression
positive regulation of secretion
positive regulation of defense response
negative regulation of immune system process
negative regulation of defense response
negative regulation of cytokine production
ncRNA processing
multicellular organismal homeostasis
monosaccharide metabolic process
lipid localization
interleukin−2 production
interleukin−1 production
interferon−gamma production
gastrulation
face development
establishment of protein localization to membrane
epithelial cell development
embryonic organ development
*defense response to other organism
cytoplasmic translation
cytokine secretion
cytokine metabolic process
cellular response to biotic stimulus
cell redox homeostasis
cell chemotaxis
aminoglycan metabolic process
adaptive immune response
IAV - + +
DI + - +
−log10(FDR)
2
3
4
Upregulated
Downregulated
2
0
−2
Normalized Enrichment Score
B
IAV infection
Monocytes
CD20+ B
CD4+ T
CD8+ T
NK
13
7
response to virus
response to type I interferon
response to interferon-beta
defense response to other organism
response to interferon-alpha
viral life cycle
regulation of multi-organism process
DI treatment IAV infection
Monocytes
CD20+ B
CD4+ T
CD8+ T
NK
16
5
response to virus
response to type I interferon
response to interferon-beta
defense response to other organism
response to interferon gamma
DI treatment uninfected
Monocytes
CD20+ B
CD4+ T
CD8+ T
NK
24
2
protein targeting
protein localization to endoplasmic reticulum
C
Lymphocytes and NK cells, GO Biological Process (FDR < 0.05)
−log10(FDR) 2 3 4
Upregulated
Downregulated
Normalized Enrichment Score 2 0 −2
viral life cycle
type I interferon production
translational initiation
T cell activation
rRNA metabolic process
RNA catabolic process
ribonucleoprotein complex subunit organization
ribonucleoprotein complex biogenesis
* response to virus
*response to type I interferon
response to nutrient levels
response to mechanical stimulus
response to interferon−gamma
*response to interferon−beta
response to interferon−alpha
response to dsRNA
regulation of response to biotic stimulus
regulation of nuclease activity
regulation of multi−organism process
regulation of leukocyte activation
regulation of innate immune response
IAV - + + - + + - + + - + +
DI + - + + - + + - + + - +
CD20+ B
CD4+ T
CD8+ T
NK
regulation of cell morphogenesis
regulation of cell−cell adhesion
regulation of binding
protein targeting
protein localization to endoplasmic reticulum
positive regulation of cell adhesion
positive regulation of cell activation
negative regulation of immune system process
membrane fusion
leukocyte cell−cell adhesion
immune response−regulating signaling pathway
fat cell differentiation
establishment of protein localization to membrane
ERK1 and ERK2 cascade
epithelial cell proliferation
* defense response to other organism
cytoplasmic translation
cell redox homeostasis
apoptotic mitochondrial changes
antigen processing and presentation
adaptive immune response
IAV - + + - + + - + + - + +
DI + - + + - + + - + + - +
CD20+ B
CD4+ T
CD8+ T
NK